Stony Brook University

Function of the Usher N- and C-Terminal Domains in Pilus Biogenesis

A Dissertation Presented by

Qinyuan Li

to

The Graduate School

in Partial Fulfillment of the

Requirements

for the Degree of

Doctor of Philosophy

in

Molecular Genetics and Microbiology

Stony Brook University

December 2009

Stony Brook University

The Graduate School

Qinyuan Li

We, the dissertation committee for the above candidate for the

Doctor of Philosophy degree, hereby recommend

acceptance of this dissertation.

David G. Thanassi, Ph.D. Dissertation Advisor

Associate Professor Department of Molecular Genetics and Microbiology

James B. Bliska, Ph.D. Chair person of Defense

Professor Department of Molecular Genetics and Microbiology

James B. Konopka, Ph.D.

Professor Department of Molecular Genetics and Microbiology

A. Wali Karzai, Ph.D.

Associate Professor Department of Biochemistry and Cell Biology

Suzanne Scarlata, Ph.D.

Professor Department of Physiology and Biophysics

This dissertation is accepted by the Graduate School

Lawrence Martin

Dean of Graduate School

Abstract of the Dissertation

Function of the Usher N- and C-Terminal Domains in Pilus Biogenesis

by

Qinyuan Li

Doctor of Philosophy

in

Molecular Genetics and Microbiology

Stony Brook University

2009

Attachment to host cells by surface adhesive structures is a prerequisite step for many pathogenic bacteria to cause disease. The adhesive P and type 1 pili are two well-studied prototype structures that are assembled by *uropathogenic Escherichia coli* (UPEC), which is by far the most common causative agent of urinary tract infections. P pili are critical virulence factors of UPEC and their assembly on the bacterial surface requires the chaperone/usher pathway. In this pathway, the periplasmic chaperone PapD facilities the folding of pilus subunits and the outer membrane usher PapC catalyzes pilus assembly and provides the channel to allow secretion of the pilus fiber to the cell surface. Many questions remain about the molecular mechanism of pilus assembly at the

usher.The usher contains four domains: 1) N-terminal domain; 2) C-terminal domain; 3) translocation domain; and 4) middle domain (plug domain). In this thesis, I investigated the structure and function of the N- and C-terminal domains of the PapC usher in P pilus biogenesis. My results from PapC C-terminal domain structure analysis by mutagenesis are consistent with a recently published PapC crystal structure. Using an antibiotic sensitivity assay, I investigated how the N- and C-terminal domains participate in controlling the gating of the PapC channel. I found that the N-terminal domain of PapC plays an important role in controlling the PapC channel activity. To investigate the molecular details of the N- and C-terminal domains in P pilus assembly, I established a new fluorescence based technique to quantify usher-chaperone-subunit interactions *in vitro.* This *in vitro* fluorescent binding assay confirmed that the chaperone-adhesin complex PapDG has the highest binding affinity for PapC. Further, I used this assay to show that PapC N-terminal mutant F21A and C-terminal mutant R652A have altered affinities for PapDG and PapDA complexes, supporting roles for the N- and C-terminal domains in the differential affinity of the usher for chaperone-subunit complexes. Finally, I investigated if the PapG adhesin is required for pilus assembly and found PapG is not required for P pilus assembly. Thus, the preferential affinity of the usher for the adhesin may ensure assembly of functional P pili.

Table of Contents

List of Tables

List of Figures

Acknowledgements

More than words

I could never reach this stage in my life without the support and help from many people during this journey.

First, I am very grateful to my advisor Dr. David G. Thanassi. I learnt a lot from Dr. Thanassi since I joined this lab five years ago. Dr. Thanassi is always very kind and patient and is willing to help me anytime. I also want to thank him for giving me the chance to join his lab and expose myself to this area of research and make learning enjoyable. Dr. Thanassi made the laboratory a very warm and comfortable place to work. I am grateful to all current and previous members of the Thanassi Lab. Especially, I thank the former member, Ken-Michael who contributed to the PapG deletion work. I greatly appreciate him, not only for preparing tons of medium and plates for my work, but also for spending a lot of time helping me purify protein. I want to thank former students Tony and Stephane, who contributed lots of work on N- and C-terminal domain of PapC usher project. I thank Stephane especially, who was the one who mentored me in the beginning stages of my project and helped me a lot with my work. I also want to thank Nadine who taught me the technique for protein purification, and for always keeping the lab organized. I also thank previous coworkers Tony and Haracio who gave me many suggestions and input for my projects.

I am grateful to my Committee Dr. James Bliska, Dr. Wali Karzai, Dr. James Konopka, and Dr. Suzanne Scarlata. I appreciate their input and useful suggestions toward my work. I especially thank Dr. Scarlata who was so kind to provide her lab facility for my fluorescence analysis.

I am grateful to all my friends I've made along the way as I pursued my Ph.D. degree. I appreciate their help and effort to make my life much easier. I would like to specially thank Ken-Michael Bayle, my best friend, who always tried his best to give me the most support and would always be there for me whenever I asked for help. I also want to thank Jie Chen, Xingyue He, Ying Zheng, Gabrielle Platz, Lisa Runco, Zhiyun Ge, Lingyin Ge and Ruixue Wang, who are like my sisters, for being so sweet to me and supportive. It was fun to have all of my friends to share different views about life and I have learned a lot from each of them. Without their friendship, my life would be very different.

I would like to specially thank my parents for their eternal support since I was born. My father and my mother sacrifice almost all of their life to support me no matter if my life was up or down. While pursuing my Ph.D. degree, they spent almost three years helping me take care of my kids. I could never reach this stage without them. My daughter Aileen and my son Andrew, who are dearest to my heart, make my life so happy and meaningful. They bring me so much joy and my heart is fulfilled just being with them. Lastly but not least, I thank a special person in my life, my husband Yi Xia, who

has spent 8 years with me, is always there for me to support me and try his best to make me happy no matter how difficult life is. I also learned a lot from him about different kinds of views concerning science and life.

Chapter 1

Introduction

I. Urinary Tract Infections (UTIs)

Urinary Tract Infections (UTIs) are one of most common bacterial infections and contribute 150 million cases worldwide annually [1]. In the United States, there are about 8 million physician visits resulting from UTIs per year [3, 4]. UTIs are the second most common bacterial infections in children and can cause renal scarring leading to secondary hypertension and chronic kidney disease. At least 10% to 20% of women and 12% of men experience UTIs during their lives [5]. In the United States, UTIs account for over 100,000 hospitalizations each year [6]. Acute pyelonephritis is a more severe but less common type of UTI, and is associated with substantial morbidity and mortality.

UTIs are bacterial infections that occur in the urinary system including kidneys, ureters, bladders and urethra. Although the urinary system is usually sterile for a healthy adult, bacterial infections commonly occur. In general, bacterial infections in the urinary tract occur in an ascending manner. Bacteria first colonize in the peri-urethral area, then ascend to the bladder causing cystitis, and finally bacteria can reach the kidneys to cause the pyelonephritis. Severe damage of the kidneys, such as scarring of the kidney, kidney failure and sepsis can be caused by untreated acute pyelonephritis. UTIs are categorized by infection sites or into complicated and uncomplicated infections: uncomplicated UTIs occur in otherwise healthy immunocompetent patients, while complicated UTIs occur in immunosuppressed patients and/or patients who have genitourinary tract obstruction or

abnormalities.

Uropathogenic *Escherichia coli* (UPEC) are the main pathogen that cause UTIs, and account for more than 75% of infections [7]. UTIs are less commonly caused by *Staphylococcus saprophyticus, Klebsiella spp., Proteus spp., Enterococcus spp.* and *Enterobacter spp.* [7]. The urinary tract has a number of defense features: the unidirectional flow of urine in the urinary tract can flush bacteria out of the host; the host immune system can prevent the bacterial proliferation; and antibodies can also inhibit extracellular pathogens [8]. However, UPEC possess certain virulent factors that are associated with the pathogenesis of the bacteria, such as adhesins, toxins, siderophores and hemolysin [9]. These factors help the pathogens to survive and overcome immune or antimicrobial factors in the host [10].

All humans are susceptible to UTIs, but certain factors increase the chance for infections. Age and gender are markers of host susceptibility to infection. In general, women are more susceptible to UTIs than men with a radio of 30:1 [11]. Almost half of adult female are affected at least once in their lifespan [12]. UTIs are more common for women during pregnancy [13]. UTI also occur more often in males older than 50, and are associated with abnormalities in the urinary tract such as prostatic enlargement [1]. Urinary catheter and vaginal intercourse are also related to developing the UTIs due to increased exposure to the pathogen in the urinary tract [6].

Antibiotics are the typical treatment for UTIs. So far, the most effective antibiotic for UTIs is fluoroquinolones [14]. However, antibiotic-resistant bacterial stains have emerged with the broad use of antibiotics. Therefore, it is important to develop novel

antibiotics in order to catch up with the newer antibiotic-resistant bacteria. One strategy to prevent UTIs is to develop a vaccine that could be used to disrupt the binding and colonization of bacteria to the host. Currently, studies are being done that focus on developing a vaccine for the FimH adhesin of UPEC to interfere with the binding of the adhesin to the host bladder epithelium to prevent cystitis caused by UPEC [15]. It is suggested that one other method to prevent the UTIs is ingestion of cranberry juice, which was shown to interfere with the attachment of bacteria to uroepithelial cells [16]. It is believed that cranberries modify urine pH and contain proanthocyanidins that limit bacterial binding to host cells [17]. Although the detailed mechanisms are not well understood yet, the development of a therapy using a natural product is another option to prevent the UTIs.

II. Virulence Factors of UPEC

Not all *E. coli* are able to cause UTIs, and the virulence factors particular to each strain are key factors which enable UPEC to cause the disease. The genes encoding virulence factors are usually clustered together in “pathogenicity islands” (PAIs) of UPEC strains [18]. The virulence factors of UPEC include adhesins, siderophores, toxins, polysaccharide coatings, invasins and proteases [19, 20]. Following is a brief description of some of them.

Adhesins

The ability of UPEC to adhere to host cells is an important step in successful

colonization of the urinary tract. Adherence to the epithelium in the urinary tract allows bacteria to overcome the unidirectional flush of the urine flow. In UPEC, the attachment of bacteria to the host epithelium is mediated by assembly of adhesive structures on the bacterial cell surface, which are known as adhesins. Adhesins recognize specific receptors on the host cell to initiate colonization and the development of disease. Most *Escherichia coli* adhesins are hair-like structures termed pili (fimbriae), but afimbrial molecules can also act as adhesins allow to colonization of the urinary tract and initiate the infectious process.

Pili (Fimbriae)

The surface hair-like structures termed fimbriae or pili are critical for colonization of the host by bacteria. The fimbrial adhesin is usually composed of polymers consisting of non-adhesive structural subunits with the adhesin on the distal end of the fiber (Fig. 1-1). The subunits interact with each other noncovalently to form pilus fibers. Among these structures are two types of well studied fimbriae, P pili and type 1 pili. The pilus rod, which is the main part of the pilus fiber, is arranged in a helical coiled structure. The coiled structure on the bacterial surface can unwind to withstand shear force during urine flow and maintain adhesion to host cells [21]. The rod structures of pili partially contribute the pathogenesis of UPEC colonizing the urinary tract [21]. In UTIs, P pili bind to receptors in the kidney, leading to the development of pyelonephritis, and type 1 pili attach to receptors in the bladder, initiating a cascade of events leading to the development of cystitis [22, 23].

P pili

P pili consist of six structural proteins that connect end-to-end to form a fiber composed of two distinct sub-assemblies: a 8 nm thick rigid helical rod and a 2 nm diameter flexible tip fiber that is located at the distal end of the rod (Fig.1-1) [24, 25]. The rod contains more than 1,000 copies of the PapA subunit and is terminated by a single copy of PapH, which may also help anchor the pilus in the bacterial outer membrane (OM) [26]. The P pilus tip contains approximately 5-10 copies of the PapE subunit, which is linked to the PapA rod via the PapK adaptor subunit. PapG is linked to PapE via the PapF adaptor subunit. The PapG adhesin is present at the distal end of the tip and binds to Galα(1-4)Gal moieties present in kidney glycolipids [22, 27].

Type 1 Pili

Type 1 pili are fibers which range from 1 μm to 3 μm in length [28]. A 7-nm-thick helical rod is mainly made of repeating FimA subunits which is connected to a 3-nm-wide tip fibrillum made of FimF and FimG adhesin (Fig. 1-1) [28]. The FimH adhesin specifically binds to D-mannose residues in glycoproteins on the epithelium of bladders [29].

Siderophore

Siderophores are essential for bacteria using iron as a nutrient within the host. *E. coli* uses iron for oxygen transport, DNA synthesis, and metabolism of peroxides [30, 31]. At least two siderophores are secreted by UPEC, enterochelin and aerobactin, to acquire

iron from the environment [30]. The strains with the aerobactin system grow faster in urine with low-iron conditions than other strains [32]. Aerobactin is more common in UPEC strains that are able to cause acute pyelonephritis [33].

Toxins

Hemolysins

Hemolysin production is associated with virulent *E. coli* in UTIs. Hemolysins can lyses erythrocytes, disrupt phagocytes, contribute cytotoxicity to host tissues, and enable bacterial persistence in animal kidneys [34-38]. Disruption of erythrocytes by hemolysin can cause anemia, which is a main complication of acute pyelonephritis [39].

Cytotoxic necrotizing factor type 1 (CNF1)

CNF1 is a member of the family of bacterial toxins that target the Rho family of small GTP-binding proteins [40]. CNF1 secreted by UPEC strains is a key player that initiates formation of actin stress fibers, filopodia and membrane ruffling [41]. The cytoskeleton rearrangement in the host cell triggered by CNF1 promotes bacterial internalization [41].

III. Secretory Pathways by Gram-negative Bacteria

Bacteria secrete different proteins with functions ranging from nutrient acquisition to assembly of surface structures. These functions are correlated with bacterial virulence. Therefore, it is important to understand detailed mechanisms of protein secretion so as to

understand bacterial pathogenesis. In addition to the inner membrane (IM), proteins destined for secretion by Gram-negative bacteria must cross the periplasm and outer membrane (OM) to reach the extracellular environment or be present on the cell surface to interact with the host cells [42]. To overcome this obstacle of crossing both membranes, Gram-negative bacteria have evolved numerous secretory machineries for protein transportation (Fig. 1-2) [43]. There are two main groups of secretory machineries: the Sec-independent and Sec-dependent pathways [43]. The Sec-independent pathways transport the protein from the cytoplasm across the IM and OM in a single step, without periplasmic intermediates. Type I and Type III secretion pathways are Sec-independent pathways, which can secrete proteins directly to the cell surface or directly inject proteins into host cells [44-46]. Type II, the autotransporter (AT or type V), two partner secretion (TPS) and chaperone/usher (CU) pathways are Sec-dependent [47-54]. The type IV pathway belongs to both categories since proteins transported via this pathway can be injected directly into host cells from the cytoplasm or periplasm [55]. Recently, a type VI secretory pathway was reported, which shares similarity to the type IV secretion system [56]. The detailed mechanism of type VI secretion is still under exploration. The source of energy is important for protein secretion across the OM in the Gram-negative bacteria since ATP is not available in the periplasm. Type I, II, III, and IV pathways take advantage of energy harnessed at the IM to export the proteins, while AT, TPS and CU pathways do not use energy available at the IM and depend on the energy from transformation of the protein folding status. The type VI secretion system is reported as ATP dependent [57].

Type I secretion (ABC)

The type I (or ABC) protein secretion system comprises an IM ATP-binding cassette (ABC) protein, an OM channel that extends across the periplasm, and a periplasmic membrane fusion protein (MFP) that links the IM and OM proteins [44]. This pathway is involved in toxin, protease and lipase secretion [58]. The type I secretion pathway is exemplified by *E. coli* alpha hemolysin. The IM ABC translocase (HlyB) recruits the OM channel TolC via the MFP (HlyD) after interaction with hemolysin to form a channel across both membranes. The energy from ATP hydrolysis by HlyB drives hemolysin secretion to the cell surface [59].

Type III secretion system (T3SS)

T3SS machineries span both the IM and OM and assemble a needle-like structure on the cell envelope. T3SS are able to secrete proteins across the bacterial OM as well as inject these proteins into the host cell [46, 60]. This pathway is exemplified by *Yersinia* outer proteins (Yops) which can be secreted directly to the host cell via the needle apparatus [61]. YopB and YopD are inserted via the needle complex into the host plasma membrane to form a channel that allows other effector Yop proteins to translocate into the cytoplasm of the host cell [62-64]. The IM ATPase YscN drives the T3SS to secrete the protein.

Type II secretion system (T2SS)

Protein secretion by the type II secretion system occurs in a Sec-dependent

manner. After translocation across the IM via the Sec general secretory machinery, the proteins fold into a translocation competent form in the periplasm and finally cross the OM. Some bacterial toxins, proteases, pectinases, lipases, and phospholipases are transported via this pathway [54]. The pullulanase (PulA) of *Klebsiella* oxytoca was the first protein identified as secreted via T2SS [65]. Before released into the extracellular medium, PulA is temporarily anchored on the cell surface via its N terminus.[66]. The cytoplasmic protein PulE acts as an ATPase and provides the energy for PulA secretion [66]. PulC was shown to bridge the OM and IM [67]. PulG, PulH, PulI and PulJ are pilin-like proteins and are thought to assemble as a pilus-like structure across the periplasm to help secretion of PulA [68]. PulD is a large integral OM protein and provides the translocation pore [69]. The PulS OM lipoprotein interacts with and directs PulD to target and insert into the OM [69].

Autotransporter (AT)

The autotransporter pathway is also defined as the type V secretion system (T5SS), which contains a protein with an N-terminal signal peptide, a passenger domain, and a C-terminal β-domain. After translocation across the IM via the Sec system and cleavage of the signal peptide, the C-terminal domain inserts into the OM and provides a channel to allow secretion of the N-terminal domain to the cell surface [47, 50, 51]. The passenger domains are released to the environment or anchor to the cell surface. This pathway is exemplified by *Neisseria gonorrhea* IgA1 protease [70]. The C-terminal domain of the AT protein NalP of *Neisseria meningitis* forms a 12-stranded β-barrel

structure in the OM containing a hydrophilic pore [71]. An α-helix linker region occupies the central channel of β-barrel with the N-terminal passenger domain exposed to the cell surface, which signifies the N-terminal domain must be in an unfolded state in the channel before the linker occupies the pore [70-74]. The N-terminal passenger domain is thought to fold when it reaches the cell surface. No energy is required for secretion across the OM in this pathway [72].

The Two-partner Secretion Pathway (TSP)

Although this pathway shares many similarities with the AT pathway, it differs from the AT pathway in having a separate OM transporter (TpsB) and secreted protein (TpsA) [52]. One main feature of this pathway is that the transporter protein and exoprotein are usually encoded in one operon or in the same locus [52]. After translocation via the Sec pathway across the IM, a periplasmic chaperone might help TpsA to across the periplasm. Recently, the X-ray structure of one TpsB transporter has been solved, with two POTRA (polypeptide-transport-associated domain) domains in the periplasm, a transmembrane β-barrel and a large loop harboring a functionally important motif [75, 76]. The conserved N-terminal domain of TpsA plays an important role in secretion and release of TpsA [47]. The N-terminal domain interacts with TpsB on the periplasm side and might trigger the channel opening of TpsB [72]. Energy is not required for secretion across the OM by this pathway and the folding of TpsA on the cell surface may drive protein secretion. The filamentous haemagglutinin (FHA) of Bordetella pertussia is transported by this pathway [77].

Chaperone/Usher Pathway (CU)

This pathway is a main pathway for secretion and assembly of adhesive surface structures [53, 72]. Two well studied prototypes of this pathway are UPEC type 1 and P pili. A periplasmic chaperone coupled with an OM usher act to secrete and assemble the proteins on the cell surface. The details of this pathway are presented below.

Type IV secretion system (T4SS)

The type IV secretion system is generally Sec-independent except with *Bordetella pertussis* toxin (PT) where secretion is Sec-dependent. The T4SS can inject proteins into host cells from either the cytoplasm or periplasm. T4SS can not only secrete proteins, but single-stranded-DNA-protein complexes as well, which is considered to be related to the bacterial conjugation system [55, 78]. The VirB system of *Arobacterium tumefaciens* is a well studied example of this pathway. The T4SS secretion apparatus is encoded by the *virB* cluster and exports the single-stranded T-DNA into plant cells. VirB2 is believed to form a pilus-like structure for translocating the substrate across the OM. VirB7 and VirB9 are localized at the OM to form a translocation pore [79]. VirB4 and VirB11 have ATPase activity to provide the energy in the IM and help the secretion of substrate proteins [80].

Type VI secretion system (T6SS)

The hallmark of T6SS is that its components are encoded with IcmF-associated homologous proteins (IAHP), the cytoplasmic membrane proteins which were previously reported in the *Legionella* T4SS [81]. However, the other gene cluster of the T6SS has no

homology with T4SS components. The secretion of hemolysin coregulated protein (Hcp) and the valine-glycine repeat protein G (VgrG) require T6SS [56, 82, 83]. After translocated cross the IM, Hcp monomer forms hexamer in the periplasm and acts as one component of T6SS machineries [84]. Several effector proteins transported by T6SS have been reported recently such as EvpP in *Edwardsiella tarda*, RbsB in *Rhizobium leguminosarum* and TssM in *Burkholderia mallei* [83, 85-87]. However, the biological significance of these effectors in T6SS has not been determined. The molecular details and precise roles of T6SS remain unknown.

IV. P Pilus Biogenesis by CU Pathway

Outer membrane proteins

The OM of Gram-negative bacteria is an asymmetric bilayer, with phospholipids in its inner leaflet and lipopolysaccharides (LPS) in its outer leaflet. The proteins in the OM are mainly divided into two classes: lipoproteins, which are anchored in the inner or outer leaflets, and integral proteins, which span the entire OM bilyer. Integral OM proteins usually contain an even number of amphipathic antiparallel ß-strands that fold into a ß-barrel with hydrophobic residues facing outwards [88]. After translocation across the IM, OM proteins interact with several periplasmic chaperones and folding catalysts, which are reported to assist their folding and insertion into the OM [89, 90]. Skp (Seventeen-kilodalton-protein) is a periplasmic chaperone which interacts with OM proteins right after they cross the IM via the Sec system [91]. SurA is a peptidyl-prolyl isomerase (PPIase), which binds to unfolded OM proteins [92, 93].

The OM Usher

OM ushers are integral ß-barrel proteins that span the whole OM region. In P and type 1 pili systems, two OM usher proteins, PapC and FimD, respectively, are synthesized as precursors with an N-terminal signal sequence and cross the IM via the Sec system [89, 94]. PapC and FimD are integral OM proteins containing 809 amino acids and 833 amino acids, respectively [95, 96]. After being inserted into the OM, PapC and FimD fold into a ß-barrel structure with a central channel (Fig.1-3) [95, 97]. The β-barrel structure is highly stable and resistant to denaturation by SDS, unless exposed to high temperature.

The usher contains four distinct domains: a transmembrane ß-barrel domain, a middle or plug domain that interrupts the ß–barrel domain, and periplasmic N- and C-terminal domains (NTD and CTD, respectively) (Fig.1-3) [2, 98, 99]. Recently, the crystal structure of the translocation domain of $PapC_{135-640}$ revealed that 24 transmembrane ß-strands span the OM and form the core ß-barrel region occluded by a middle domain (plug domain) (Fig.1-3) [2]. The channel of the PapC usher is large enough to allow secretion of a linear fiber of folded pilus subunits, but in the resting usher, the channel is gated by the internal plug domain [2, 100]. The X-ray structures of the FimD NTD and NTD-FimCH complex were also recently solved (Fig. 1-4) [101]. The NTD forms a soluble, globular domain in the periplasm. High-resolution electron microscopy studies demonstrated that PapC forms twin-pore dimer complexes and functions asymmetrically [2, 100, 102]. In pilus biogenesis, the OM usher is a platform that catalyzes the pilus assembly correctly.

Pilus biogenesis by chaperone/usher pathway

P and type 1 pili are prototype fibers assembled by CU secretion pathway, which is used by many Gram-negative bacteria for the assembly of virulence-associated surface structures [53]. The P and type 1 pili are encoded by the *pap* and *fim* gene clusters, respectively, and their expression is highly regulated with ON/OFF phase variation (Fig.1-1) [103]. PapI and PapB are regulatory proteins that control expression of the Pap proteins [104]. The FimB and FimE recombinases act on an invertible DNA switch region which is located between the *fimE* and *fimA* genes to control the expression of Fim structural and assembly proteins [105, 106].

Pilus assembly by the CU pathway requires two specialized assembly factors known as the periplasmic chaperone (PapD for P pili) and OM usher (PapC for P pili). Following translocation across the cytoplasmic membrane via the Sec general secretory pathway [107], P pilus subunits must interact with the PapD periplasmic chaperone [107]. The P pilus subunits misfold or aggregate and will be degraded by the periplasmic DegP protease in the absence of chaperone [108]. Pilus subunits contain an incomplete immunoglobulin (Ig)-like fold termed the pilin domain. However, the pilin domain is missing the seventh ß-strand that is present in canonical Ig folds [29, 109-111]. The missing strand results in a deep groove on the surface of the subunit and exposes a hydrophobic groove. The chaperone facilities the folding of pilus subunits by donating a β-strand to complete the subunit pilin domain, in a mechanism termed donor strand complementation (DSC) [24, 29, 109, 111]. DSC also results in the capping of interactive surfaces to prevent premature subunit-subunit interactions and maintains subunits in an

assembly competent state. Periplasmic chaperone-subunit complexes next must interact with the OM usher. The usher catalyzes subunit assembly into the pilus fiber and provides the channel for secretion of the fiber to the cell surface (Fig.1-5) [112-114]. Interaction of chaperone-subunit complexes with the usher promotes chaperone release, in a process that is coupled with formation of subunit-subunit interactions [115, 116]. Pilus subunits contain a conserved N-terminal extension (Nte) in addition to the pilin domain. Subunit-subunit interactions form when the Nte from an incoming chaperone-subunit complex displaces the donated chaperone ß-strand from the preceding chaperone-subunit complex, completing the Ig fold of the preceding subunit in a mechanism termed donor strand exchange (DSE) [109, 110]. Thus, the pilus fiber is built from an array of Ig folds, with each subunit bound to the preceding subunit by DSE. Note that the adhesin, which is located at the tip of the pilus fiber, contains an N-terminal adhesin domain in place of the Nte. DSE allows subunits to adopt a lower energy state compared to DSC with the chaperone; the exchange of chaperone-subunit for subunit-subunit interactions is thought to energize pilus biogenesis at the usher [110, 117].

The NTD of the PapC usher serves as the initial binding site for chaperone-subunit complexes, and the CTD stabilizes this binding (Fig.1-4B) [4, 101, 118]. The pilus assembles in a specific order and in a top down manner. The pilus adhesin is incorporated first, followed by the tip fibrillum and finally the rod. The usher differentiates among the chaperone-subunit complexes to ensure that pilus fiber assembly occurs in the correct order according to the final position of the subunits in the pilus [119, 120].

V. Current Model for P Pilus Assembly

According to previous studies, we found that the PapC NTD serves as the initial binding site for chaperone-subunit complexes [4], and is involved in discriminating different chaperone-subunit complexes by direct binding to chaperone-bound subunits in the periplasmic side [101]. The CTD is required for pilus assembly [118], and plays an important role after binding of chaperone-subunit complexes to the NTD [118].

To combine these findings with previous EM studies and the recent crystal structure of the PapC usher, the proposed model for P pilus assembly is described here (Fig.1-5): The PapDG chaperone-adhesin complex first targets to the NTD of one usher of the twin-pore usher dimer. Binding of the chaperone-adhesin complex is stabilized by the usher CTD, and binding of PapDG triggers a conformational change of the usher, which somehow induces the channel opening of the usher by rotation or displacement of plug domain [2, 118, 119]. The next chaperone-subunit complex, PapDF, targets to the NTD of the other usher; the channel of this usher remains closed because only the chaperone-adhesin complex was shown to open the usher channel [119]. The NTD of the usher has a flexible linker at the periplasmic side so that it can bring PapDF next to the previously bound PapDG [2]. The two chaperone-subunit complexes are now positioned next to each other to form the first link of the pilus fiber by DSE [110]. The chaperone PapD is dissociated from PapG after the formation of the first subunit-subunit interaction and the NTD of the first usher is also detached from PapG and is now available for the next chaperone-subunit complex, PapDE. The process repeats and the NTDs alternately recruit chaperone-subunit complexes from the periplasm so that the pilus assembles in

order and crosses the OM through the usher channel. Once the pilus reaches the cell surface, the adhesin PapG can recognize Galα1-4Gal on the epithelial cells in the kidneys.

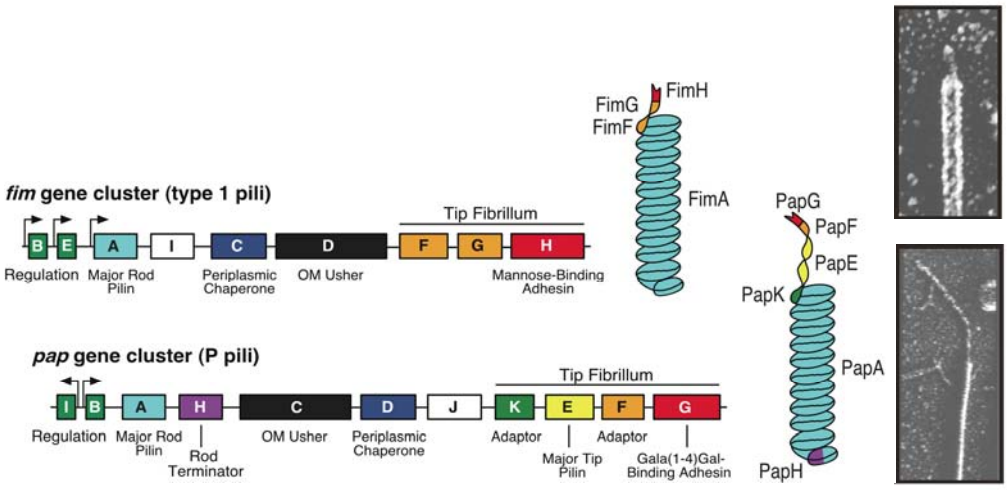

Thanassi, (2002) J. Mol. Microbiol. Biotechnol. 4(1): 11-20

Fig. 1-1. Schematic representation of the *pap* and *fim* gene clusters. Schematic representation of the *pap* and *fim* gene clusters coding for P and type 1 pili coding for P and type 1 pili, respectively. Cartoons of the assembled P pilus and type 1 pilus are shown, along with corresponding electron micrographs.

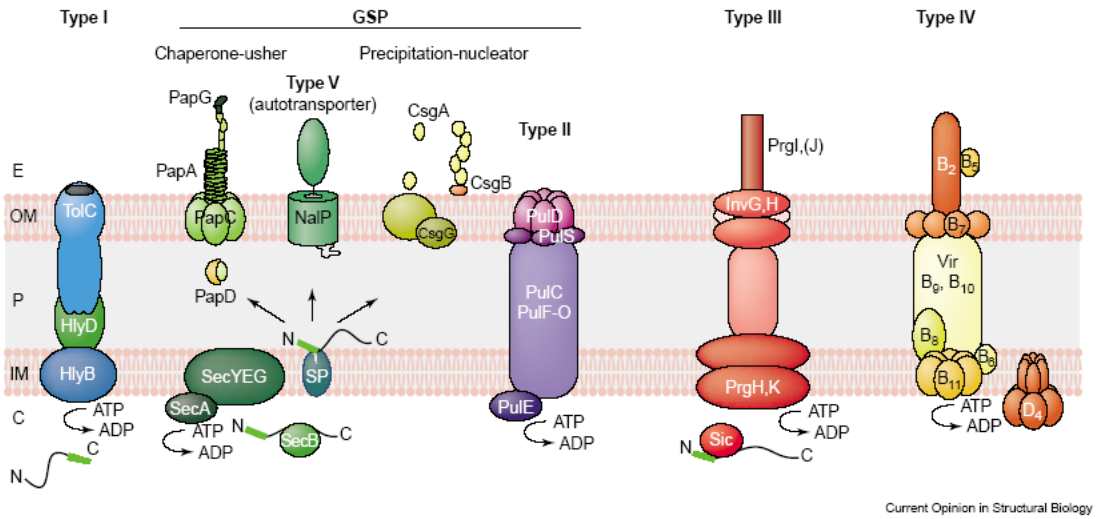

Remaut and Waksman, (2004) Curr. Op. Struct. Biol. Vol. 14 p.161

Fig. 1-2. Secretory machineries in Gram-negative bacteria. Proteins are synthesized in the cytoplasm (C) and then transported across the inner membrane (IM), periplasm (P), and outer membrane (OM), and finally secreted to the extracellular space (E). The secretory machineries can be divided into two pathways, Sec-dependent and Sec-independent pathways. Sec-dependent pathways require the Sec machinery for protein translocation through the IM and have a periplasmic intermediate that must be secreted across the OM. Proteins secreted by the Sec-independent pathways can be directly transported from the cytoplasm across the OM.

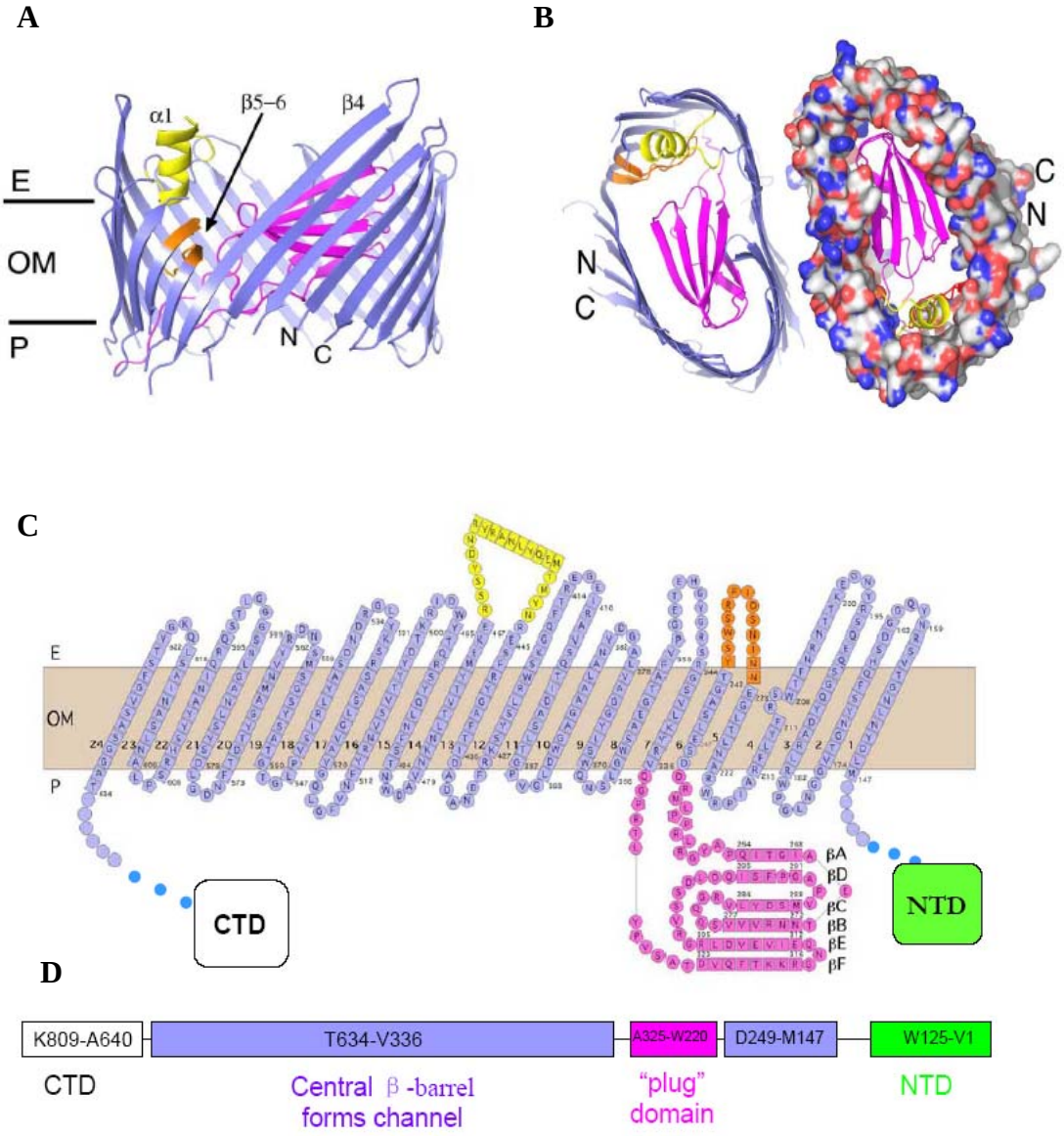

Fig. 1-3. Crystal structure [2] and topology of PapC. (A) Crystal structure of $PapC_{130\text{-}640}$ viewed from the side. (B) $PapC_{130\text{-}640}$ translocation channel viewed from the extracellular side. (C) PapC topology indicated with the N-and C-terminal domains on the periplasmic side, β-barrel domain (blue ribbon) and plug domain (magneta) (D) Schematic representation of each domain corresponding to the amino acids of PapC. Adapted from Remaut *et. al.*, (2008) Cell, 133(4): p.640-52

A

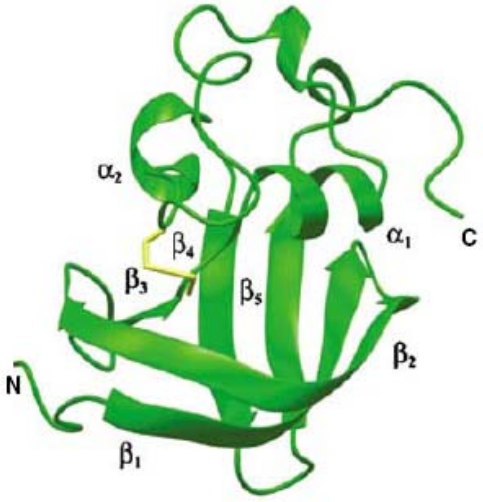

B

Nishiyama et.al. 2005. EMBO, 24, 2075-2086.

Fig. 1-4. X-ray structure of NTD of FimD (A) X-ray structure of FimDN (25-125). **(B)** X-ray structure of the ternary FimDN(1–125)–FimC–FimHP complex.

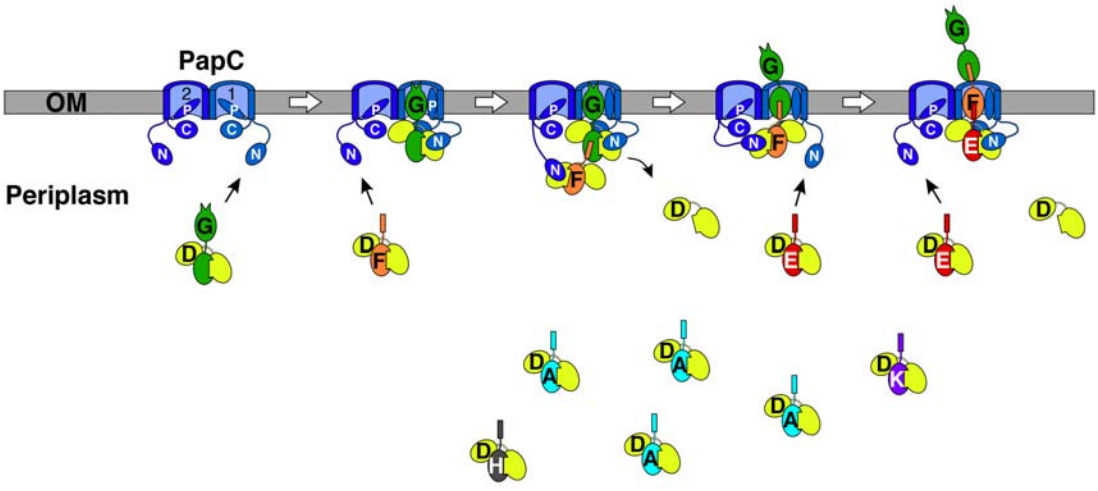

Fig. 1-5. Current proposed model of pilus biogenesis. See text for details.

Chapter 2

Materials and Methods

Strains and plasmids. The strains and plasmids used in this study are listed in Table 2-1. All strains were grown at 37°C with aeration in Luria-Bertani (LB) medium with appropriate antibiotics. The primers used for mutagenesis are listed in Table 2-3 and Table 2-4. Plasmid pMJ3 was created previously [4], and encodes *papC* under the control of the arabinose (P_{ara}) promoter. The PapC substitution mutations plasmid pTN51 (PapC F18A), pTN52 (PapC F21A), pSS21 (PapC R652A) and pSS2 (PapC C787S) were derived from pMJ3 using the QuikChange site-directed mutagenesis kit (Stratagene, La Jolla, Calif.) and DH5α as the host strain. Plasmid pQY_{21} was derived from pTN52 (PapC F21A) using the QuikChange site-directed mutagenesis kit to insert a thrombin cleavage site between the C-terminus and His-tag. pPapDA is vector pBAD18 carrying PapDA under an arabinose inducible promoter. pDGT10, pSSR652A, pSSF21A are wild-type PapC, mutant PapC R652A, and mutant PapC F21A, respectively, in pACYC184 under an IPTG inducible promoter. pPap58 is PapDJKEFG in pMMB91 vector with an IPTG-inducible promoter. pDG2 was previously created [100], and encodes *papC* with a thrombin cleavage site connected to a His-tag. pNH200 carries *papD* derived from pHJ9210 with a thrombin cleavage site between the C-terminus and His-tag.

The plasmids harboring PapC deletion mutants or substitution mutants were derived from pMJ3 using the QuikChange site-directed mutagenesis kit. All the

plasmids were transformed to DH5 α as host strain. The primers used to construct the mutations are listed in Table 2-5. All mutations were confirmed by sequencing.

Constucting *papG* deletion mutant. Plasmid pPapΔG, a *papG* deletion mutant, was derived from plasmid pPap5 which has the complete *pap* gene cluster cloned into the medium copy number vector pBR322 under control of the native *pap* promoter [27]. A BamHI restriction site in the intergenic region between *papF* and *papG* was inserted in pPap5 using the QuikChange™ (Stratagene) mutagenesis kit. The whole *papG* gene was deleted by digesting the pPap5-BamHI mutant with BamHI and religating to create the plasmid pPAPΔG. The *papG* chromosomal deletion in bacterial strain ZAP594 was constructed by the λ Red Recombinase system [121]. The primers designed for deletion of *papG* are shown in Table 2-3. The Kanamycin resistance cassette with flanking FRT sites from plasmid pKD4 was amplified by polymerase chain reaction (PCR) by the following parameters: denaturation at 94°C for 7 min, 26 cycles of denaturation at 94°C for 1 min, annealing at 58°C for 45 s, and extension at 72°C for 1 min 40 s, followed by a final elongation step at 72 °C for 10 min. The PCR product was purified and then transformed into the ZAP594 strain harboring the λ Red Recombinase expression vector pKD46 by electroporation. Kanamycin-resistant transformants of ZAP594 were screened by PCR to confirm replacement of the targeted gene with the kanamycin cassette. The kanamycin cassette was then eliminated by the FLP recombinase expression vector, pCP20. The final constructs were confirmed by PCR. pHGM98, which encodes the *papI* regulator gene, was then

transformed into the Δ*papG* mutant strain and wild type ZAP594 strain to increase the transition of off-to-on *pap* operon [122].

Outer Membrane (OM) Isolation. OM was isolated as previously described [95] using a SF100 or Tuner strain. Bacteria were induced, harvested, washed, and resuspended in Tris-HCl (pH 8.0) containing Complete protease inhibitor cocktail (Roche, Indianapolis, N.Y.) followed by passage through French press (SLM Instruments, Rochester, N.Y.) at 14,000 lb/in^2. The unbroken cells were removed by centrifugation (30 min, 10,000 x g, 4℃). 0.5% Sarkosyl (sodium-N-lauroylsarcosinate; Sigma, St. Louis, MO.) was added to selectively dissolve the inner membrane by rocking for 5 min at room temperture. The OM was then pelleted by ultracentrifugation (80,000 x g, 65 min, 4°C) and resuspended in 20 mM Tris (pH 8.0)-0.3 M NaCl.

Hemagglutination assays (HA). Hemagglutination assays were performed by serial dilution in microtiter plates as previously described [99], with *E. coli* strain AAEC185 as the host. The bacteria were induced, washed and adjusted to OD540 of 1.0 in PBS. 3 ml of this bacterial suspension were resuspended in 100 µl PBS. Human red blood cells were washed and adjusted to OD640 of 1.9. HA were performed in 96-well V-bottom microtiter plates containing 25 µl of serial 2-fold dilutions of each bacterial suspension and 25 µl of red blood cells. The plates were then store at 4°C overnight and the highest bacterial dilution that was still able to cause agglutination of human

red blood cells was recorded. Assays for assembly of adhesive complete P pili were performed using host strain AAEC185/pMJ2 and assays for assembly of adhesive P pilus tips were performed using host strain AAEC185/pPAP58. Assays for assembly of adhesive complete P pili in PapG deletion mutants were performed using AAEC185 as host strain.

Isolation of pili. P pili isolation was carried out by heat extraction and magnesium precipitation as described previously [99]. The pilus isolation from AAEC185/pMJ2 host strain harboring PapC mutants was conducted by growing 100 ml cultures, followed by induction with 0.1% arabinose and 50 μM IPTG. For the Δ*papG* mutants, new bacterial strains AAEC185 containing vector, pPap5, or pPAPΔG, or the chromosomal *papG* deletion in strain ZAP594 with or without pHGM98 were grown on the CFA (colonization factor antigen) agar plates for 3 passages at 37°C. Next, bacteria were harvested, washed and then adjusted equally at OD540. Equal volumes of the suspension were centrifuged and resuspended into 1 ml of 5 mM Tris(pH 8.0)-75 mM NaCl. Samples were heated at 65°C for 30 min to release P pili from the bacterial surface. The samples were centrifuged (6,000 x g, 5 min, 4°C) after cooling down to room temperature. The supernatants were then transferred and centrifuged again (16,000 x g, 20 min, 4 °C). The pili were precipitated by adding 0.25 ml of 1 M NaCl and 0.35 ml of 0.5 M $MgCl_2$. The samples were rocked for 2 hours at room temperature, and pili were pellet by centrifugation (16,000 x g, 30min, 4°C). To break up the subunit-subunit interactions, purified pili were acidified with 4 mM HCl

in SDS sample buffer and then were incubated (95°C, 10 min), followed by neutralizing with 4 mM NaOH. The samples were then subjected to SDS-PAGE. The major rod components (PapA) were detected by Coomassie blue staining. P pilus tip proteins (PapEFG) were detected by blotting with anti-P pilus tip antisera. The blots were developed with the appropriate alkaline phosphatase-conjugated secondary antibody and BCIP (5-bromo-4-chloro-3-indolylphosphate)-NBT (nitroblue tetrazolium) substrate (KPL).

Transmission Electron Microscopy (TEM). Bacterial strains were grown, induced, washed and resuspended with phosphate-buffered saline (PBS). Bacteria were allowed to adhere to Formvar carbon-coated electron microscopy (EM) grids (Ernest F. Fullam, Latham, N.Y.) for 2 min and then fixed on the grids with 1% glutaraldehyde in PBS for 1 min, washed twice with PBS briefly, washed twice with water for 1 min, and stained for 20 s with 0.5% phosphotungstic acid. The grids were examined on a FEI BioTwinG^2 Transmission Electron Microscopy (FEI^{TM}, Hillsboro, Oregon) at an 80-kV accelerating voltage.

Periplasm preparation. Periplasm preparation was performed as previously described [4]. Bacteria were induced, harvested, washed, and resuspended followed by adding 0.1 μM EDTA and 75 μg/ml lysozyme. 0.2 μM of MgCl2 was added to the mixture after 40 min incubation on ice. The samples were then centrifuged (9,000 x g, 20 min, 4°C) after 20min incubation on ice. Supernatant fractions (periplasm)

containing chaperone-subunit complexes were collected and stored at 4°C.

Characterization of the PapC NTD mutants. The PapC F18A and F21A constructs were compared with WT PapC for expression level in the OM by immunoblotting with anti-His-tag (Covance) or anti-PapC antibodies. Immunoblots were developed with the appropriate alkaline phosphatase-conjugated secondary antibody and BCIP-NBT substrate. Strain SF100 harboring vector control (pMON6235Δcat), WT PapC (pMJ3) or a PapC NTD mutant (pTN51 or pTN52) was induced at OD600 = 0.6 with 0.1% l-arabinose for 1 h, and OM fractions were isolated by French press disruption and Sarkosyl extraction, as described [4, 118]. Proper folding of the PapC constructs in the OM was checked by resistance to denaturation by SDS, which provides an indication of proper folding and stability of the ß-barrel domain [119]. This was determined by heat-modifiable mobility on SDS-PAGE, performed as described [4, 118].

Effect of PapDA expression on pilus biogenesis by the PapC F21A and R652A mutants. Hemagglutination assays and purification of pili from the bacterial surface were performed as described above, with the following modifications. Host strain AAEC185/pPAP58 (papDJKEFG) + pPAPDA (papDA) harboring vector control (pACYC184), WT PapC (pDGT10) or one of the PapC mutants (pSSF21A or pSSR652A) was induced with 0.1 mM IPTG (for expression of PapC and the pilus tip subunits) and either 0, 0.05, 0.1 or 0.5% l-arabinose (for expression of PapDA). The

controlled expression of PapA in response to arabinose was confirmed by isolation of periplasm fractions, as described [4], and analysis by SDS-PAGE and Coomassie blue staining or immunoblotting with anti-PapA antiserum.

Protein Purifications. The PapC ushers were purified as follows. OM fractions were isolated as described above from strain SF100 harboring WT PapC (pDG2), PapC Δ2-11 (pTN35), PapC F21A (pQY21) or PapC R652A (pQY652). The OM was solubilized by resuspending in 20 mM Tris-HCl (pH 8), 0.12 M NaCl and 1% dodecyl-maltopyranoside (DDM; Anatrace), and rocking overnight at 4ºC. Insoluble material was removed by centrifugation (80,000 g, 45 min, 4ºC), imadazole was added to 20 mM to the supernatant fraction and this fraction was run over a nickel affinity column (HisTrap; GE Healthcare) using an Akta FPLC apparatus (GE Healthcare). The bound PapC protein was eluted using an imidazole step gradient in buffer A [20 mM Tris-HCl (pH 8), 0.12 M NaCl and 10 mM lauryl(dimethyl)amine oxide (LDAO; Anatrace)]. Fractions containing PapC were pooled and the His-tag was cleaved off PapC by overnight digestion at room temperature with 10 units thrombin per mg PapC while dialyzing against 20 mM Tris-HCl (pH 8) and 0.12 M NaCl. The thrombin was inhibited by addition of PMSF and the mixture was subjected to a second round of chromatography in buffer A using a HisTrap column directly linked to a HiTrap benzamidine column (GE Healthcare). In this case, the thrombin-cleaved PapC came off the columns in the flow-through fraction, whereas uncleaved PapC, contaminants and the thrombin remained bound to the columns.

The collected flow-through material was dialyzed into 20 mM Hepes (pH 7.5), 150 mM NaCl and 5 mM LDAO, and concentrated using a Millipore Ultrafree centrifugal concentrator (50 kDa molecular weight cutoff). Protein concentrations were determined using the bicinchoninic acid (BCA) protein assay (Pierce).

The PapD chaperone and PapDG chaperone-adhesin complex were purified as follows. Strains Tuner/pNH200 (His-tagged PapD) and Tuner/pNH200 + pTN17 (PapG) were induced with 0.01% l-arabinose for PapD expression and 1 mM IPTG for PapG expression, and periplasm fractions were isolated as described [4]. The periplasms were dialyzed into 20 mM Tris (pH 8) and 0.3 M NaCl, imidazole was added to 20 mM, and the samples were run over a nickel affinity column (HisTrap) using an Akta FPLC apparatus. The bound proteins were eluted using an imidazole step gradient, and fractions containing the purified PapD or PapDG were dialyzed into 20 mM MES (pH 5.8). The samples were then subjected to an additional chromatography step using a Resource S ion exchange column (GE Healthcare) and eluted using a NaCl gradient. The purified PapDAs were supplied by Dr. Karen Dodson from Dr. Hultgren Lab.

In vitro fluorescence-based assay for quantification chaperone-subunit binding to the usher. Measurements of binding affinities to the usher were conducted essentially as described [123]. Purified chaperone or chaperone-subunit complexes were labeled with the amine-reactive probe coumarin SE (DMACA, SE; Invitrogen). For labeling, the pH of the protein solution was first raised to 8.0 by addition of

K_2HPO_4, and then probe was added at a 5:1 probe:protein molar ratio and the mixture incubated for 45 min at 4ºC. A final concentration of 1 mM 2-mercaptoethanol was then added to inactivate unreacted probe, and the solution was dialyzed at 4°C against at least 3 changes of 20 mM Hepes (pH 7.5), 150 mM NaCl to remove unreacted probe, followed by a final overnight dialysis against 20 mM Hepes (pH 7.5), 150 mM NaCl and 5 mM LDAO to put the labeled proteins into the same buffer as the purified PapC. The labeling efficiency was checked by comparing protein absorbance at 280 nm with absorbance of the probe at 376 nm.

Fluorescence measurements were performed at room temperature using a PC1 photon counting spectrofluorometer (ISS). The coumarin-labeled chaperone or chaperone-subunit complex was diluted to 25 nM final concentration using 20 mM Hepes (pH 7.5), 150 mM NaCl and 5 mM LDAO, and 120 µl was transferred to a 3 mm microcuvette. Purified PapC was then titrated into the cuvette and spectra were recorded using a 376 nm excitation wavelength and by scanning emission values from 420 to 520 nm. The area under the curve was calculated to give the total emission intensity. Corrections for background scatter were made by subtracting out intensity values obtained by titrating with buffer only, and corrections for dilution were made to account for changes in volume during PapC titration. The values were normalized to present the data as the fraction of protein bound as a function of added PapC, with the starting value (no PapC added) set to 0 and the final value (highest concentration of PapC added) set to 1. Apparent dissociation constants (Kd) were then obtained by fitting the data to a titration curve using the sigmoidal curve-fitting function in

SigmaPlot (Systat Software). Each titration curve represents the average of at least three independent experiments, with one-to-three replicates per experiment.

Overlay assay. This assay was described previously [120]. OM was isolated as described above and was mixed with an equal volume of 2x SDS sample buffer, incubated at 95°C for 12 min, subjected to SDS-PAGE, and transferred to PVDF (Osmonics, Westborough, MA). The membrane was blocked overnight with 5% milk in buffer A (10 mM Tris [pH 8.0], 0.5 M NaCl, 0.5% Tween 20). Periplasm preparations isolated as described above, were diluted with an equal volume of buffer A and incubated with the PVDF membrane for 2 h. The membrane was washed three times in buffer A. Binding of chaperone-subunit complexes to the proteins on the membrane was determined by immunoblotting with anti-PapDG antibody or anti-P pilus tip antisera, followed by an alkaline phosphatase-conjugated secondary antibody. The blot was developed with BCIP-NBT substrate.

Top soft agar assay for antibiotics sensitivity. Bacteria were added to the soft top agar which is made of 0.75% agar. The bacteria and melted agar were mixed well and poured on the top of 1.5% solid agar plates. Next, 6 mm discs containing 10 µl of the following antibiotics were placed on the top: 750 mg/ml SDS, 20 mg/ml vancomycin, 15 mg/ml erythromycin, 5 mg/ml rifampicin or 30 mg/ml novobiocin. The inhibition zone of the antibiotics was measured after growing the plates overnight at 37℃. Bacterial strains expressing different truncation mutants were compared in this assay, which

includes the PapCΔ1-128 (ΔN), PapCΔ641-809(ΔC) and PapCΔ1-128,641-809 (ΔN,ΔC). The bacterial strain containing wild type PapC usher was used as a positive control and empty vector was used as a negative control.

Colony-forming unit (CFU) assay for antibiotic sensitivity. The bacteria were grown overnight and then were diluted to 1:100 on the following day, followed by adding 0.001% arabinose. 15 μg/ml erythromycin, 30 μg/ml vancomycin or 0.025% SDS was added into the liquid culture after 30 minutes induction. After 17 hours growth, the bacteria were serially diluted to spread on the agar plates containing ampicinlin and incubated at 37℃ overnight. On the following day, colony forming units (CFU) were determined by counting the colonies on the plates. The averages presented (log_{10} CFU per ml) were derived from at least 3 independent experiments

Co-purification of PapC with chaperone-subunit complexes. Bacterial strain SF100 harboring pJP1 (PapDG under control of IPTG) or pMJ5 (PapDF under control of IPTG) was transformed with pMJ3 (His-tagged PapC wild type) or pTN37 (His-tagged PapC C70A). Strains were grown in 100 ml of LB broth containing appropriate antibiotics at 37°C with aeration, and then induced at an OD600 of 0.6 for 1 h by addition of 0.1% L-arabinose and 100 μM IPTG. The OM fractions were isolated as described above. The OM pellet was resuspended in 1 ml of 20 mM Tris-HCl (pH 7.5)-0.3 M NaCl and solublized with 0.5% n-dodecyl-ß-D-maltoside (DDM; Anatrace, Maumee, Ohio) by rocking overnight at 4°C. Unsolublized OM was

removed by centrifugation (100,000 x g, 45 min, 4°C). Next, solublized OM containing a final concentration of 20 mM imidazole was loaded onto a high performance HisTrap nickel column (GE Healthcare, Piscataway, N.J.) with buffer A (20 mM Tris-HCl [pH 7.5], 0.15 M NaCl, 0.05% DDM, 20 mM imidazole) by Pharmacia Akta-fast-performance liquid chromatography apparatus (GE Healthcare, Piscataway, N.J.). The step gradient of 10% buffer B (20 mM Tris-HCl [pH 7.5], 0.15 M NaCl, 0.05% DDM, 0.4M imidazole) was performed to removed the contaminants and the final His-tagged PapC was eluted from the nickel column with 60% buffer B. The elutions were subjected to SDS-PAGE and blotted with anti-P pilus tips antisera. Blots were developed with an alkaline phosphatase-conjugated secondary antibody and BCIP-NBT substrate.

Table 2-1. Strains and plasmids used in this study

Strains or plasmids	Relevant characteristic(s)c	Reference
Strains		
Tuner	B strain *ΔompT Δlon*	Novagen, Madison, WI
DH5α	*hsdR recA endA*	[124]
SF100	*ΔompT*	[125]
AAEC185	MM294*Δfim* (lacking entire *fim* gene cluster)	[126]
ZAP594	Allelic exchange of papJ96 F13 cluster from pLD1 in AAEC090A	[122]
Plasmids:		
pMON6235Δcat	Vector, $P_{ara,}$ Amp^r	[108]
pMMB91	Vector; P_{trc} Kan^r	[120]
pMMB66	Vector; P_{ara} Amp^r	[119]
pACYC184	Vector; P_{trc} Tet^r	[97]
pMJ3	PapC-His in pMON6235Δcat	[97]
pPAP58	PapDJKEFG in pMMB91 vector, P_{trc} Kan^r	[127]
pTN52	PapC F21A in pMJ3, P_{ara} Amp^r	This study

pTN5	PapC C70A in pMJ3, P_{ara} Amp^r	[4]
pAP3	PapCΔ2-11 in pMJ3, P_{ara} Amp^r	[4]
pSS21	PapC R652A in pMJ3 P_{ara} Amp^r	[118]
pQY_{21}	PapC F21A with thrombin cleavage site site/His tag, P_{ara} Amp^r	This study
pQY_{652}	PapC R652A with thrombin cleavage site site/His tag, P_{ara} Amp^r	This study
pTN35	PapCΔ2-11 with thrombin cleavage site/His tag, P_{ara} Amp^r	[4]
pTN37	PapC C70A with thrombin cleavage site/His tag, P_{ara} Amp^r	[4]
pDGT10	PapC wild type in pACYC184, P_{trc} Tet^r	This study
pSSR652A	PapC R652A in pACYC184, P_{trc} Tet^r	This study
pPapDA	PapDA in pBAD-18, P_{ara} Clm^r	This study
pDG2	PapC wild type with thrombin cleavage site/His tag. P_{ara} Amp^r	[128]
pNH200	PapD with thrombin cleavage site /His tag	[128]
pTN17	pMMB66 with PapG, P_{trc} Amp^r	This study
pTK5	pMMB66 with PapK, P_{trc} Amp^r	This study
pJP1	*papDG* in pMMB91; $kan^{r;}$ P_{trc}	This study
pMJ4	*papDK* in pMMB91; kan^r; P_{trc}	This study
pMJ5	*papDF* in pMMB91; kan^r; P_{trc}	This study

pPap5	plasmid encolde entire pap gene cluster	[27]
pPapΔG	*papG* deletion in pPap5	This study
pPap24	Truncating >60% *papG* at a *Bgl*II site of pPap5 Amp^r	[129]
pKD4	Kan^r cassette with flanking FRT sites	[121]
pKD46	λ Red Recombinase genes (γ,β,exo)	[121]
pCP20	FLP Recombinase	[130]
pHGM98	pACYC184 with inducible papI, $P_{tcr,}Tet^r$	[122]
pQY_1	PapCΔ588-623 in pMJ3, P_{ara} ,Amp^r	This study
pQY_2	PapCΔ588-599 in pMJ3, P_{ara} ,Amp^r	This study
pQY_3	PapCΔ600-609 in pMJ3, P_{ara} ,Amp^r	This study
pQY_4	PapCΔ610-619 in pMJ3, P_{ara} ,Amp^r	This study
pQY_5	PapCΔ632-674 in pMJ3, P_{ara} ,Amp^r	This study
pQY_6	PapCΔ640-649 in pMJ3, P_{ara} ,Amp^r	This study
pQY_7	PapCΔ650-659 in pMJ3, P_{ara} ,Amp^r	This study
pQY_8	PapCΔ660-669 in pMJ3, P_{ara} ,Amp^r	This study
pQY_9	PapCΔ791-800 in pMJ3, P_{ara} ,Amp^r	This study
pQY_{789}	PapC V789A in pMJ3, P_{ara} ,Amp^r	This study
pQY_{791}	PapC V791A in pMJ3, P_{ara} ,Amp^r	This study
pQY_{792}	PapC P792A in pMJ3, P_{ara} ,Amp^r	This study

pQY_{794}	PapC T794A in pMJ3, P_{ara} ,Amp^r	This study
pQY_{795}	PapC I795A in pMJ3, P_{ara} ,Amp^r	This study
pQY_{796}	PapC S796A in pMJ3, P_{ara} ,Amp^r	This study
pQY_{801}	PapC L801A in pMJ3, P_{ara} ,Amp^r	This study
pQY_{802}	PapC L802A in pMJ3, P_{ara} ,Amp^r	This study
pQY_{803}	PapC L803A in pMJ3, P_{ara} ,Amp^r	This study
pQY_{804}	PapC P804A in pMJ3, P_{ara} ,Amp^r	This study

All strains are *E.coli* K-12, except Tuner, which is *E. coli* B strain.

P_{ara}, arabinose-inducible promoter; P_{trc}, IPTG-inducible promoter; Amp^r,ampicillin resistance; kan^r, kanamycin resistance; Clm^r, chloramphenicol resistance. .

Table 2-2. Primers used to delete *papG*

Primer	Sequence (5'-3')
ZAP594-G-FOR	TGGTTACGGAGTGACAGCAG
ZAP594-pap5-REV	CAGCCAGTCAGATAATCCATCA
Homo-G-For	ATGAAAAAATGGTTCCCTGCTTTTTTATTTTTATCCC TGTCAGGCGGTAA GTGTAGGCTG GAGCTGCTTC
Homo-G-Rev	TCAGGGGAAACTCAGAACCATAGTCATAGAACCAG ATAGC TCCCCGGGTT CATATGAATA TCCTCCTTAG

Table 2-3. Primers for insertion of Thrombin digestion site.

C/throm/F	CTGTACGCCTCAGAAACTGGTCCCCCG GGGCAGCCATCACCATCACCATC
C/throm/R	GATGGTGATGGTGATGGCTGCCCCGGGGGACCAGT TTCTGAGGCGTACAG

Table 2-4. Primers used to make PapC mutants.

V789A-F	GGAAAAATACAGTGTCAGGCAAATGTACCGGAGACAGC
V789A-R	GCTGTCTCCGGTACATTTGCCTGACACTGTATTTTTCC
V791A-F	CAGTGTCAGGTAAATGCACCGGAGACAGCAATATC
V791A-R	GATATTGCTGTCTCCGGTGCATTTACCTGACACTG
P792A-F	CAGTGTCAGGTAAATGTAGCAGAGACAGCAATATCTGAC CAG
P792A-R	CTGGTCAGATATTGCTGTCTCTGCTACATTTACCTGACAC TG
T794A-F	CAGGTAAATGTACCGGAGGCAGCAATATCTGACCAG
T794A-R	CTGGTCAGATATTGCTGCCTCCGGTACATTTACCTG
I795A-F	GTACCGGAGACAGCAGCATCTGACCAGCAGTTATTGC
I795A-R	GCAATAACTGCTGGTCAGATGCTGCTGTCTCCGGTAC
S796A-F	CCGGAGACAGCAATAGCAGACCAGCAGTTATTGCTTCCC
S796A-R	GGGAAGCAATAACTGCTGGTCTGCTATTGCTGTCTCCGG
L801A-F	GCAATATCTGACCAGCAGGCATTGCTTCCCTGTACGCC
L801A-R	GGCGTACAGGGAAGCAATGCCTGCTGGTCAGATATTGC
L802-F	GCAATATCTGACCAGCAGTTAGCACTTCCCTGTACGCCT CAG
L802-R	CTGAGGCGTACAGGGAAGTGCTAACAATAACTGCTGGT CAG
L803-F	CTGACCAGCAGTTATTGGCACCCTGTACTGCTGGTCAGA

	TATATTGC
L803-R	CATTTATTTCTGAGGCGTACAGGGTGCCAATAACTGCTG GTCAG
P804-F	CTGACCAGCAGTTATTGCTTGCATGTACGCCTCAGAAAT AAATG
P804-R	CATTTATTTCTGAGGCGTACATGCAAGCAATAACTGCTGG TCAG
DE632-674-F	GTCAGTGCTTCCGGTTGGGGAACGGGC
DE632-674-R	GCCCGTTCCCCAACCGGAAGCACTGAC
DE640-649F	CCGGAAAAGGTGGAACACGTCTTCTTGTTGAC
DE640-649R	GTCAACAAGAAGACGTGTTCCACCTTTTCCGG
DE650-659F	GGAATGTCCGGTGTGGGAGGTGTACCG
DE650-659R	CGGTACACCTCCCACACCGGACATTCC
DE660-669F	GTTGACACGGATGGTGTGGTGACAAATCGC
DE660-669R	GCGATTTGTCACCACACCATCCGTGTCAAC
DE588-623F	CCGGCCTTAACTCTTTCGGCGTCAGTG
DE588-623R	CACTGACGCCGAAAGAGTTAAGGCCGG
DE588-599F	GCCGGCCTTAACGCCTATTACAGTCATCG
DE588-599R	CGATGACTGTAATAGGCGTTAAGGCCGGC
DE600-609F	CATCGCAACGTCAGATTAATAATTTGTCCGCG
DE600-609R	CGCGGACAAATTATTAATCTGACGTTGCGATG
DE610-619F	CTGAGTCCGCTGGCAAAAGGATATACGTCTTTC

DE610-619R	GAAAGACGTATATCCTTTTGCCAGCGGACTACG
DE791-800F	CAGTGTCAGGTAAATTTATTGTTGCTTCCCTGTACGCCT
DE791-800R	AGGCGTACAGGGAAGCAATAAATTTACCTGACACTG

Chapter 3

In vitro analysis of usher-chaperone-subunit interactions

Abstract

Attachment to host cells via adhesive surface structures is a prerequisite for the pathogenesis of many bacteria. UPEC, the predominant causative agent of urinary tract infections, assembles P and type 1 pili for attachment to the host urothelium. Assembly of these pili requires the conserved CU pathway. In this pathway, a periplasmic chaperone controls the folding of pilus subunits and an OM usher provides a platform for pilus assembly and secretion to the cell surface. The usher has differential affinity for chaperone-subunit complexes, with highest affinity for the tip-localized adhesin (PapG for P pili). This differential affinity is thought to aid in ordered pilus assembly. Residue R652 in the CTD of PapC was previously identified as required for pilus biogenesis and potentially functioning in the differential affinity of the usher. Here, we show that residue F21, located in the PapC N-terminal domain, performs a similar function. Quantitative in vitro measurements confirmed that the PapC F21A and R652A mutants have altered binding affinities for chaperone-subunit complexes. The mutants have distinct phenotypes, suggesting different roles for the N- and C-terminal domains in the ability of the usher to discriminate among chaperone-subunit complexes. The altered affinities of the PapC mutants provide an explanation for the pilus assembly defects of these mutants, which are incapable of assembling complete pili, but are capable of assembling pilus tips in

the absence of the PapA rod subunit. Analysis of PapG deletion mutants demonstrated that the adhesin is not required for P pilus biogenesis. Thus, the preferential affinity of the usher for the adhesin may ensure assembly of functional P pili.

Introduction

The PapC usher is an integral OM protein containing 809 amino acids. The usher contains four distinct domains: a transmembrane ß-barrel domain, a middle or plug domain that interrupts the β-barrel domain, and periplasmic N- and C-terminal domains (NTD and CTD, respectively) (Fig. 1-3) [2, 98, 99]. The translocation channel is formed by the ß-barrel domain, which contains 24 transmembrane ß-strands and forms a kidney-shaped channel of 3 by 4 nm internal diameter [2, 100]. This channel is large enough to allow secretion of a linear fiber of folded pilus subunits, but in the resting usher, the channel is gated shut by the internal plug domain [2]. The NTD provides the initial binding site for periplasmic chaperone-subunit complexes [4, 101] and the CTD is required for subsequent pilus assembly events [99]. The CTD contributes to the binding of chaperone-subunit complexes and may also participate in controlling access to the usher channel [118]. The usher functions in the OM as a dimeric complex, but only one channel is used for secretion of the pilus fiber [2, 100, 118]. The usher dimer may be required for successive round of recruitment of chaperone-subunit complexes from the periplasm and to facilitate positioning of the subunits for DSE (Fig 1-5) [2, 102].

Pili are assembled in a defined order, with the adhesin incorporated first,

followed by the rest of the tip fiber and finally the pilus rod. Each subunit specifically interacts with its appropriate neighbor subunit in the pilus fiber, with the specificity of binding determined by the DSE reaction [131, 132]. In addition, the usher facilitates ordered assembly by differentially recognizing chaperone-subunit complexes according to their final position in the pilus [119, 120]. Thus, the chaperone-adhesin complex binds to the usher with both highest affinity and fastest association rate compared to other chaperone-subunit complexes [119], ensuring that the adhesin is the first subunit incorporated into the pilus. The mechanism whereby the usher discriminates among chaperone-subunit complexes is not understood. The usher NTD directly binds chaperone-subunit complexes [4, 101] and the isolated NTD of the type 1 pilus usher, FimD, retains differential affinity for chaperone-subunit complexes [98]. Thus, the NTD clearly participates in discrimination among chaperone-subunit complexes. The usher CTD is also important for interactions with chaperone-subunit complexes and the isolated PapC CTD was shown to directly bind PapDG chaperone-adhesin complexes [118]. This suggests that the CTD may also participate in the differential affinity of the usher, an idea supported by the phenotype of PapC R652A and C787S mutants, which are defective for pilus biogenesis but capable of assembling pilus tip fibers when the PapA rod subunit is absent (Table 3-1) [118].

In this study, we investigated the mechanism of the NTD and CTD in the differential affinity of usher for chaperone-subunit complexes. We identified a PapC NTD mutation, F21A (Table 3-1), with a similar phenotype to the PapC R652A and

C787S CTD mutations (Table 3-1). Further, we confirmed that pilus biogenesis by both the NTD and CTD mutants is specifically inhibited by the presence of the PapA rod subunit, suggesting defects in subunit recognition and recruitment to the usher. Using an *in vitro* fluorescence-based assay, we confirmed that both mutants have altered binding affinities for chaperone-rod subunit complexes. In contrast, the PapC R652A mutant has greatly decreased affinity for PapDG and slightly decreased affinity for PapDA. These results are discussed in relation to the phenotypes of the mutants, the specific functions of the NTD and CTD, and the CU pathway assembly model. Finally, we investigated whether the PapG adhesin is required to initiate P pilus biogenesis. In the type 1 pilus system, the FimH adhesin is required to initiate pilus assembly [112, 118, 133, 134]. However, studies with P pili suggested that the PapG adhesin is not required for pilus assembly, and that the PapF and PapK tip subunits may act as initiators instead [25, 135, 136]. Here, we constructed complete deletions of papG from pap gene clusters carried on a plasmid or encoded in the chromosome. Analysis of these *papG* deletion strains showed that PapG is not required for P pilus biogenesis. Thus, the preferential affinity of the usher for the adhesin may be particularly important for P pilus biogenesis, to ensure assembly of adhesive organelles.

Results

A PapC F21A mutant is defective for assembly of complete pili, but able to assemble pilus tip fibers. The usher NTD provides the initial binding site for

chaperone-subunit complexes [4, 101]. A co-crystal structure of the FimD NTD bound to a chaperone-subunit complex revealed that the first 24 residues of FimD specifically interact with the bound complex and that three phenylalanines within this region (F4, F8 and F22) make direct contacts (Fig. 1-4) [101]. Mutation of these residues to alanine rendered FimD partly (F8A) or completely (F4A and F22A) unable to assemble type 1 pili, and the F4A and F8A mutations prevented the FimD NTD from binding chaperone-subunit complexes in vitro [101]. Within the PapC NTD, residues F3 and F21 are conserved with FimD residues F4 and F22, respectively (Fig. 3-1). PapC does not have a phenylalanine corresponding to FimD F8, but contains an additional phenylalanine at position 18 (Fig. 3-1). In agreement with the FimD data, we previously demonstrated that PapC residues 2-11 are required for the usher to bind chaperone-subunit complexes and assemble pili, and that PapC F3 is the critical residue within this region [4]. To determine if PapC F18 and F21 might be similarly important for pilus biogenesis, we constructed alanine substitution mutations of these residues. The PapC F18A and F21A mutants were expressed at similar levels in the OM compared to WT PapC and the mutations did not affect folding of the ushers, as assessed by resistance to denaturation by SDS (data not shown). The ability of the PapC mutants to complement a Δ*papC* operon for assembly of adhesive P pili was tested by the hemagglutination assay. As shown in Table 3-2, whereas bacteria expressing PapC F18A showed only a slight decrease in agglutination of human red blood cells compared to WT PapC, the F21A mutant had no agglutination activity, which was similar to the vector and PapC Δ2-11 negative controls. Purification of pili

from these bacteria by heat extraction and magnesium precipitation confirmed that the hemagglutination defect of PapC F21A was due to a loss of pilus assembly on the bacterial surface (Fig. 3-3). In contrast, the F18A mutant assembled pili similar to WT PapC, although at reduced levels in accordance with the hemagglutination results. This data demonstrates that residue F21, but not F18, is critical for pilus assembly by PapC.

To probe the basis for the defect of the PapC F21A mutant, we examined its ability to bind PapDG chaperone-adhesin complexes using an in vitro overlay assay. Interestingly, the F21A mutant retained ability to bind PapDG, although the amount of protein bound was reduced compared to WT PapC and the F18A mutant (Fig. 3-3A). In contrast, PapC Δ2-11 and the vector control were unable to bind PapDG (Fig. 3-3A), as shown previously [4]. Thus, although PapC F21 is required for pilus biogenesis, its function is distinct from the role of the NTD in binding chaperone-subunit complexes. To confirm that PapC F21A could interact with chaperone-subunit complexes *in vivo*, we analyzed the ability of the usher to co-purify with pilus tip subunits (PapDJKEFG) when expressed together in bacteria. As shown in Fig. 3-3B, pilus tip subunits co-purified with PapC F21A similar to WT PapC and PapC F18A, although at reduced levels. This was in contrast to the PapC Δ2-11 and the vector control, for which no subunits co-purified. Since PapC F21A was able to bind pilus tip subunits in vivo, we asked whether this mutant was capable of assembling functional P pilus tip fibers, using the hemagglutination assay. When co-expressed with pilus tip subunits (PapDJKEFG), the F21A mutant showed only a

slight decrease in agglutination of human red blood cells compared to WT PapC and the F18A mutant (Table 3-2), indicating that PapC F21A is functional for assembly of pilus tips. Therefore, although PapC F21A was unable to assemble pilus fibers on the bacterial surface when used to complement the complete *pap* operon (Fig. 3-2), this mutant was essentially fully functional for assembling pilus fibers when the PapA rod subunit was absent (Table 3-2).

PapC F21A and R652A mutants are specifically defective for pilus assembly in the presence of the PapA rod subunit. The phenotype of the F21A mutation in the PapC NTD closely matches the phenotype previously determined for a R652A mutation in the CTD [118]. PapC R652A was also unable to assemble complete pili, but able to bind chaperone-subunit complexes and assemble functional P pilus tip fibers in the absence of PapA. Based on this phenotype, we proposed that R652 might be important for the differential affinity of the usher for chaperone-subunit complexes [118]. PapA is present at ~1,000 or more copies per pilus, compared to only one or a few copies of the pilus tip subunits, and PapDA complexes are present at much higher concentration in the periplasm relative to the other chaperone-subunit complexes [24, 26]. Despite this, PapDG targets first to the usher to initiate pilus biogenesis due to its higher affinity [119, 120]. If the F21A and R652A mutations weaken affinity of the usher for PapDG and/or enhance affinity for PapDA, this might allow the high concentrations of PapDA in the periplasm to outcompete PapDG for binding to PapC, blocking initiation of pilus assembly. However, in the absence of PapA, assembly of

pilus tip fibers would proceed normally, as the pilus tip subunits are present at similar concentrations.

To test this model, we constructed strains harboring the PapC usher and pilus tip subunits under control of an IPTG-inducible promoter, and harboring PapDA complexes under control of an arabinose-inducible promoter. Therefore, in the presence of IPTG and the absence of arabinose, only pilus tip fibers will be assembled. Addition of increasing amounts of arabinose can then be used to control the expression of PapDA, and shift from assembly of pilus tips to assembly of complete pili. Using this experimental system, we found no changes in hemagglutination titer upon addition of arabinose for bacteria expressing WT PapC (Fig. 3-4). In contrast, for bacteria expressing PapC F21A or R652A, addition of increasing amounts of arabinose led to a corresponding decrease in hemagglutination titer (Fig. 3-4). Analysis of periplasm fractions from these strains confirmed the response of PapDA protein levels to addition of arabinose (data not shown). In addition, purification of pili from the bacterial surface confirmed that the hemagglutination titers reflected the assembly of pili on the bacterial surface; i.e., WT PapC assembled complete pili upon addition of arabinose, but only low levels pili could be purified from the mutants (data not shown). This data provides support for our proposed model that residues F21 and R652 of PapC are important for the ability of the usher to discriminate among chaperone-subunit complexes and initiate pilus assembly in the face of high PapDA concentrations in the periplasm.

Measurements of usher-chaperone-subunit binding affinity in vitro. To directly measure the binding affinity of the PapC F21A and R652A mutants for chaperone-subunit complexes, we developed an in vitro fluorescence-based assay, using purified PapDG or PapDA complexes and full-length PapC usher. The binding of PapDG chaperone-adhesin complex to the PapC usher was investigated first. The PapC protein was incrementally added to a cuvette containing coumarin-labeled PapDG. The changes in fluorescent intensity were monitored and used to plot a titration curve for PapDG binding to WT PapC, or to the alanine substitution F21A or R652A mutants of PapC (Fig. 3-5A). The titration curves showed that PapDG bound to PapC WT, mutants F21A and R652A with calculated apparent dissociation constants of 59 $\pm$ 10 nM, 62 $\pm$ 7 nM and 1593 $\pm$ 447 nM, respectively (Table 3-3). These results showed that the PapC F21A is not defective in binding affinity to PapDG chaperone-adhesin complex whereas the PapC R652A has significantly decreased binding affinity. As a control, the labeled PapD was titrated with PapC and the result showed that PapD was not able to bind to PapC under same experimental conditions (data not shown). The PapC mutant PapC Δ2-11, which lacks the initial targeting site for chaperone-subunit complexes, was also investigated as a control, and the results showed that PapDG was not able to bind to PapC Δ2-11 under the same experimental conditions (data not shown).

We next investigated the binding affinity of PapC F21A and PapC R652A to PapDA complexes. For this assay, the N-terminal extension (Nte) of the PapA subunit was replaced with the Nte of PapK (knte) to prevent oligomerization of the PapA

subunits. Titration of WT or mutant PapC into coumarin-labeled $PapDA_{knte}$ complexes showed that PapC F21A has increased binding affinity for $PapDA_{knte}$, with apparent Kd value of 648 $\pm$ 18 nM, compared to WT PapC with apparent Kd value of 1527 $\pm$ 104 nM (Fig. 3-5B and Table 3-3). However, the apparent Kd value of PapC mutant PapC R652A with $PapDA_{knte}$ is 2520 $\pm$ 32 nM, which showed that R652A has decreased binding affinity to $PapDA_{knte}$ (Fig. 3-5B and Table 3-3). These fluorescence binding assays confirmed that the PapC mutant F21A and R652A have altered binding affinity to chaperone-subunit complexes. The interpretation of these results in related to the phenotypes of the mutants is presented in the Discussion.

The PapG adhesin is not required for P pilus assembly. Previous studies demonstrated that in the type 1 pilus system, the FimH adhesin is required to initiate pilus assembly [118, 133, 134]. Binding of FimH to FimD appears to trigger a conformational change in the usher to open the usher channel and initiate type 1 pilus assembly. However, previous studies with the *pap* operon suggested that PapG is not required to initiate P pilus assembly [136], and the subunits PapF and PapK may instead act as initiators for pilus biogenesis [25, 135, 137]. To explore if the PapG adhesin is required in P pilus assembly as an initiator, we made *papG* deletion mutants and analyzed if the deletion mutants are able to assemble P pili. A previous PapG deletion mutant was made by digestion of plasmid pPap5 with BglII and BamHI, and relighting to create plasmid pPap24, containing a partial PapG deletion (Fig. 3-6). Considering that the partial deletion mutant of PapG leaves the N-terminal

adhesin domain intact, I constructed a complete deletion of the PapG adhesin in the *pap* gene cluster of pPap5 by insertion of a BamHI restriction site in the intergenic region between *papF* and *papG* and then digesting with BamHI and religating to create plasmid pPapΔG. As expected, bacteria harboring pPapΔG were not able to cause agglutination of human red blood cells by HA compared to the strong binding activity exhibited by the wild type *pap* cluster (Fig. 3-7A). Pilus isolation showed equal amounts of pilus subunits were detected from both wild type pPap5, pPap24 and the pPapΔG deletion construct (Fig. 3-7A). EM analysis of these bacteria was in agreement with the pilus purification results, and showed both *papG* deletion mutants assembled similar levels of P pili on the bacterial surface as wild type (Fig. 3-8A and Fig. 3-8B). Thus, PapG does not appear to be required to initiate assembly of P pili.

To exclude the possibility of artifacts caused by over-expression of the *pap* gene cluster from the multi-copy plasmid, we constructed a *papG* deletion in the chromosomal *pap* gene cluster of strain ZAP594 [122] using the phage λ Red recombination system. Strain ZAP594Δ*papG*, harboring pHGM98 which encodes the PapI regulator to turn on the *pap* operon expression, was able to assemble P pili similar to the parental strain. The EM analysis was in agreement with the pilus purification results, which showed both *papG* deletion mutants assembled similar levels of P pili on the bacterial surface as wild type (Fig. 3-7B, Fig. 3-8C and Fig. 3-8D).

Discussion

Protein secretion across the bacterial OM is a critical event for the virulence of Gram-negative bacteria. So far, the molecular details of pilus biogenesis at the OM are not well understood. A recently solved crystal structure and EM study showed that the PapC usher assembles as a dimer [2, 100]. The PapC usher has four predicted domains: NTD, CTD, plug domain and β-barrel domain. Previous studies showed that the NTD is the initial targeting site for chaperone-subunit complexes and the CTD is required for subsequent steps in P pilus biogenesis [4, 101, 118]. The PapC usher catalyzes pilus assembly and selectively recruits chaperone-subunit complexes to the OM to ensure the order of pilus fiber assembly on the cell surface. We investigated usher-chaperone-subunit interactions at the OM usher during pilus assembly by the CU pathway. The PapC usher has been shown to differentiate among chaperone-subunit complexes during the process of pilus assembly [118, 120] and the chaperone-subunit complexes binding affinity to PapC is correlated to the final order of P pilus assembly on the cell surface. Here, we developed a fluorescence-based method to quantitatively measure the usher-chaperone-subunit interactions. Our results suggest that the PapC NTD and CTD might regulate the ordered targeting of chaperone-subunit complexes to assemble the pili on the cell surface. It was previously reported that by ELISA and surface plasmon resonance-based assays that PapDG has the highest binding affinity for the PapC usher [119, 120]. The Kd value of PapDG binding to PapC was reported as 90 nm by surface plasmon resonance [119]. Using our assay, we found that the PapDG chaperone-adhesin complex bound to the PapC usher with apparent Kd of 59 $\pm$ 11 nM, which is similar to the previously

published value [119]. In our assay, PapDA bound with apparent Kd of 1527 ± 104 nM, which is also consistent with the previously reported value of 1500 nM by surface plasmon resonance [119]. Each pilus contains about 1,000 copies of the PapA rod subunit compared with only one PapG adhesin subunit and the PapDA complexes are present at a much higher concentration in the periplasm compared to PapDG [24, 26, 138]. Our assay showed the binding affinity of PapDA to PapC is about 20- to 30-fold lower than the binding affinity of PapDG. In addition, PapDF and PapDE have been shown to have lower binding affinity to PapC compared to PapDG. Thus, even though PapDG is present at low number compared to PapDA in the periplasm, PapDG has the highest binding affinity to the PapC usher to ensure that the PapG is the first subunit to be assembled into the pilus fiber.

A previous and the current mutagenesis study suggested that PapC residues F21 and R652 might play a role in differentiating among chaperone-subunit complexes [118]. The PapA expression assay here showed that PapC mutants F21A and R652A were not able to assemble complete adhesive pili in the presence of PapDA chaperone-rod-subunit complexes, while they were able to assemble adhesive pilus tips in the absence of rod subunits. We used a fluorescence-based assay to investigate the binding of PapC mutants F21A and R652A to PapDG or $PapDA_{knte}$. Compared to WT PapC, the PapC F21A has 2-fold higher binding affinity to $PapDA_{knte}$. These results suggest that the PapC F21A pilus assembly defect might due to increased binding affinity to PapDA. We propose that in the process of pilus assembly, the increased PapDA binding affinity in this mutant allows PapDA to

outcompete PapDG and prevents the PapDG chaperone-adhesin from targeting to the NTD of PapC. However, in the absence of PapDA, PapDG could target to usher to form pilus tips. In contrast to PapC F21A, the titration results showed that PapC R652A has decreased binding affinity to both PapDG and PapDA. According to the apparent Kd values, PapC R652A has 2-fold lowered binding affinity to $PapDA_{knte}$, but has about 30-fold lower binding affinity to PapDG compared to WT PapC. The binding affinity of PapC R652A to PapDG is dramatically decreased compared to wild type PapC, which leads to an overall effect of this mutant to have a relatively higher binding affinity to PapDA. As we previously proposed that in the process of pilus assembly, the increased PapDA binding affinity in this mutant allows PapDA to outcompete PapDG and prevents the PapDG chaperone-adhesin from targeting to the NTD of PapC whereas in the absence of PapDA, PapDG could target to usher to form pilus tips. Thus, the titration result suggests that PapC R652 is important in the stable binding of PapDG. The distinct changes in binding affinities of the PapC F21A and R652A mutants suggests that the NTD appears to be more important for differentiation among chaperone-subunit complexes whereas the CTD is more important for high affinity binding of PapDG. The results here are in agreement with previous results showing that the NTD forms the initial binding site for chaperone-subunit complexes, whereas the CTD is important in a subsequent step and is able to directly bind to PapDG [119].

In the type 1 pilus system, the FimH adhesin is required for type 1 pilus assembly [119]. Binding of the chaperone-adhesin complex FimCH to the FimD usher

stabilizes the usher in an assembly-competent conformation and allows initiation of pilus assembly. However, our results here with analysis of PapG deletion mutants showed that in the P pilus system, the PapG adhesin is not required for P pilus assembly, which suggests that the mechanism of P pilus biogenesis is different from the type 1 pilus assembly. The P pilus adhesin PapG is located at the distal end of the pilus fiber and plays the crucial role in allowing colonization. Previously, it was shown that the P pilus assembly depended on PapF and PapK since *papF*- *papK*-double mutation abolishes pilus assembly [136], which suggested that the pilus fiber assembly is not initiated by PapG adhesin but PapF and PapK. Although PapG is not required for P pilus assembly, it's the first subunit to be assembled and contributes to the colonization of virulence of the bacteria. Thus, the assembly of PapG especially relies on the affinity to PapC so that PapG could be the first subunit in the pilus fiber. Thus, proper assembly of adhesive P pili may depend upon the preferential affinity of the usher for PapG.

Table 3-1. Three classes of PapC mutants.

Class	PapC	Complete Pili	[a]Tips	Bind to chaperone- subunit complexes
I	F3A	None	None	None
	2-11	None	None	None
II	C70A	None	None	PapDG
	C97A	None	None	PapDG
	C70A+C97A	None	None	PapDG
III	F21A	None	+	PapDG, PapDE, PapDF, PapDK
	R652A	None	+	PapDG, PapDE, PapDF, PapDK
	C787S	None	+	PapDG, PapDE, PapDF, PapDK

[a]Tips: the PapC mutant is not able to ("None") or is able to ("+") assemble pilus tips.

Table 3-2. Assembly of adhesive pili by PapC mutants. The HA was conducted separately for the NTD and CTD mutants. (T. Ng and S. So, unpublished data)

PapC	[a]HA titer – pili (PapAHDJKEFG)	[a]HA titer – tips (PapDJKEFG)
Vector	0	0
WT	256	256
R652A	0	128

PapC	[a]HA titer – pili (PapAHDJKEFG)	[a]HA titer – tips (PapDJKEFG)
Vector	0	0
WT	64	1024
Δ2-11	0	0
F18A	32	1024
F21A	0	256

[a]HA titer is the highest fold dilution of bacteria able to agglutinate human red blood cells.

Table 3-3. Apparent Kd values for PapDG and PapDA binding to WT and mutant PapC ushers.

DG	WT	Kd = 59 $\pm$ 11nM
	F21A	Kd = 62 $\pm$ 7 nM
	R652A	Kd = 1593 $\pm$ 447 nM
DA	WT	Kd =1527 $\pm$ 104 nM
	F21A	Kd = 648 $\pm$ 18nM
	R652A	Kd = 2520 $\pm$ 32nM

Fig. 3-1. Alignment of the PapC and FimD N-terminal domain. The sequence alignment of the PapC and FimD NTD. The F3, F18 and F21 of the PapC usher are highlighted with yellow. Adapted from Nishiyama et.al. 2005. EMBO, 24, 2075-2086.

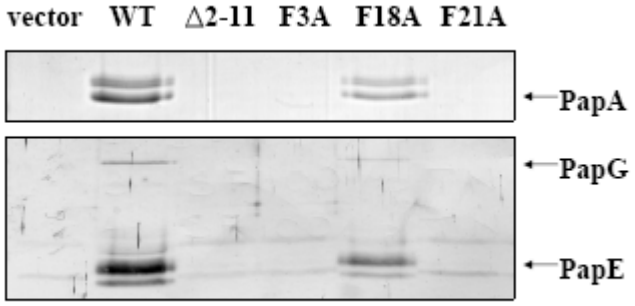

Fig. 3-2. Pilus isolation. Assembly of pili by PapC mutants. Pili assembled by strain AAEC185/pMJ2 complemented with vector, wild-type or the indicated PapC mutants. Pili were isolated from the bacterial surface by heat extraction and magnesium precipitation, and then subjected to SDS-PAGE. The PapA rod subunit was visualized by Coomassie Blue staining (upper panel). The PapE tip fibrillum subunits were detected by immunoblotting with anti-P pilus tip antibody (lower panel). The PapC Δ2-11, F3A and F21A were nonfunctional for pilus biogenesis. PapC F18A has slight defects in pilus biogenesis. (T. Ng, unpublished data).

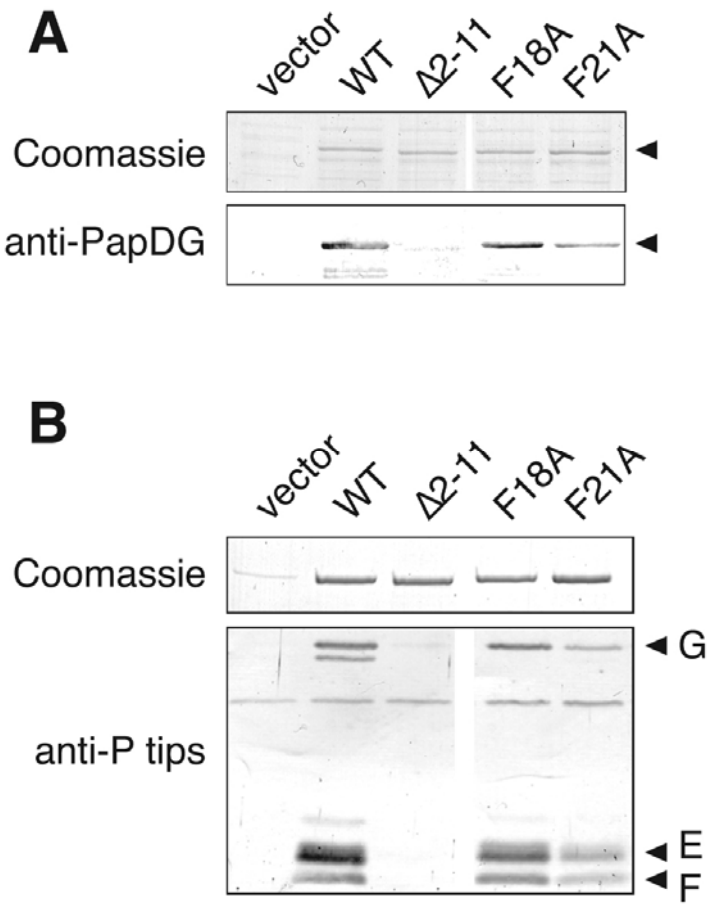

Fig. 3-3. Analysis of pilus biogenesis by the phenylalanine to alanine substituted PapC mutants. (A) Overlay assay for binding of PapDG chaperone-adhesin complexes to PapC. OM was isolated from SF100 expressing the vector alone, WT PapC, PapC Δ2-11, or the phenylalanine substitution mutants F18A or F21A. Samples were separated by SDS-PAGE and either stained with Coomassie blue to show the amount of PapC loaded (top panel) or transferred to PVDF membrane for the overlay assay (bottom panel). **(B)** Co-purification of P pilus tip subunits with the PapC usher. OM was isolated from strain SF100/pPAP58 (*papDJKEFG*) expressing the vector alone, WT PapC, PapC Δ2-11, or the phenylalanine substitution mutants F18A or F21A. OM was solubilized with DDM and PapC was purified by nickel affinity chromatography. The eluted fractions were subjected to SDS-PAGE and stained with Coomassie blue to detect purified PapC (upper panel), or immunoblotted with anti-P pilus tip antibody (bottom panel). PapC F18A and F21A are able to bind PapDG complex. The PapCΔ2-11 is not able to bind PapDG. These mutants were analyzed together with the WT PapC and vector controls (T. Ng,unpublished data)

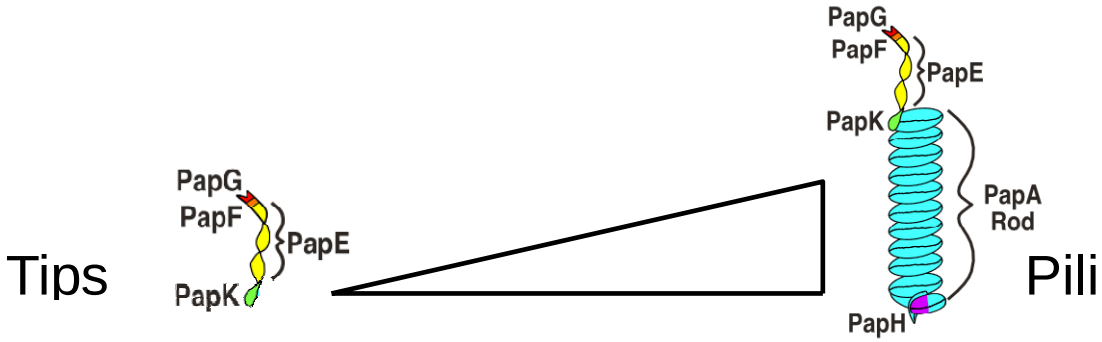

HA Titer: Pilus Tips + PapDA Under Arabinose

PapC	ARABINOSE			
	0%	0.05%	0.1%	0.5%
vector	0	0	0	0
WT	256	256	256	256
R652A	128	64	16	8
F21A	128	64	4	n.d.

Fig. 3-4. Hemagglutination assays. HA were performed in host strain AAEC185/pPAP58 (*papDJKEFG*) + pPAPDA (*papDA*) harboring vector, WT PapC, PapC F21A or PapC R652A. The bacteria were induced with 0.1 mM IPTG (for expression of PapC and the pilus tip subunits) and either 0, 0.05, 0.1 or 0.5% arabinose (for expression of PapDA). The HA titer of PapC R652A and F21A are decreasing with the increase of PapDA expression.(S. So, unpublished data).

A

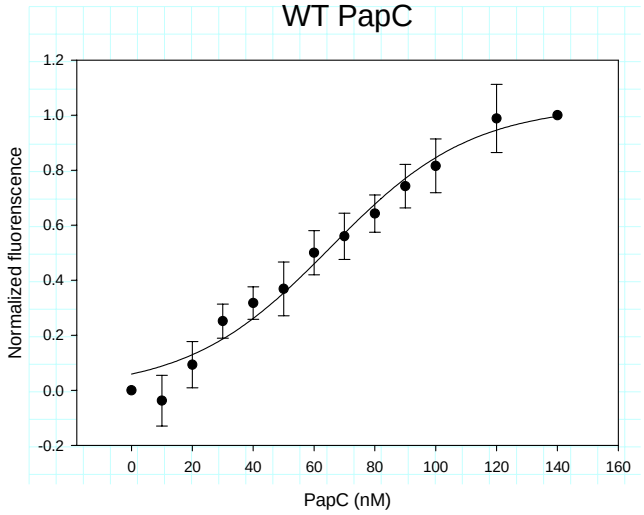
WT PapC
Normalized fluorenscence
PapC (nM)

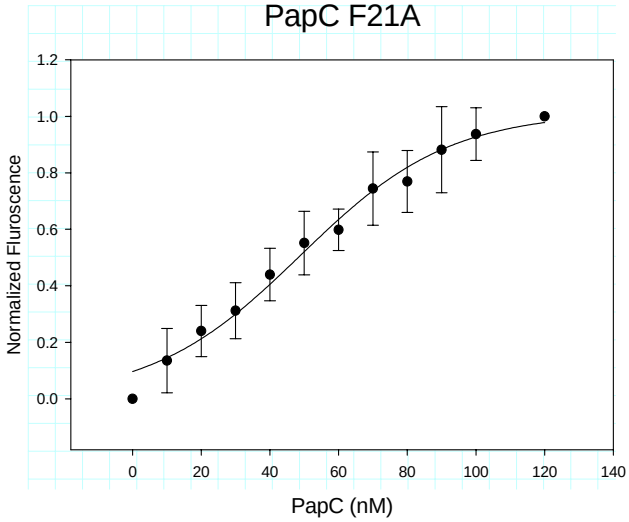
PapC F21A
Normalized Fluroscence
PapC (nM)

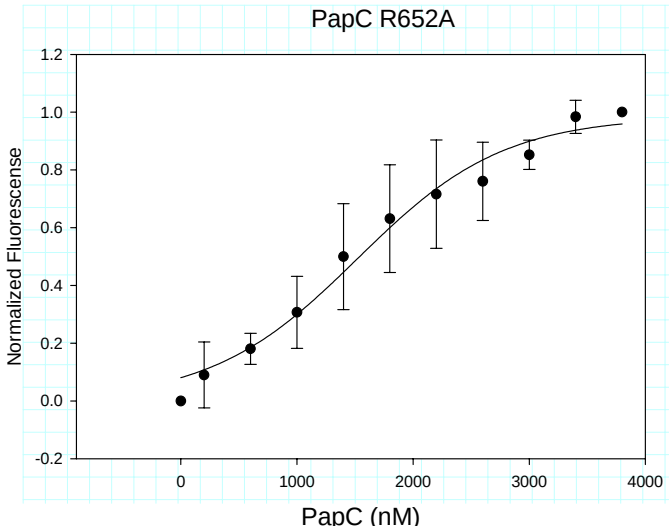
PapC R652A
Normalized Fluorescense
PapC (nM)

B

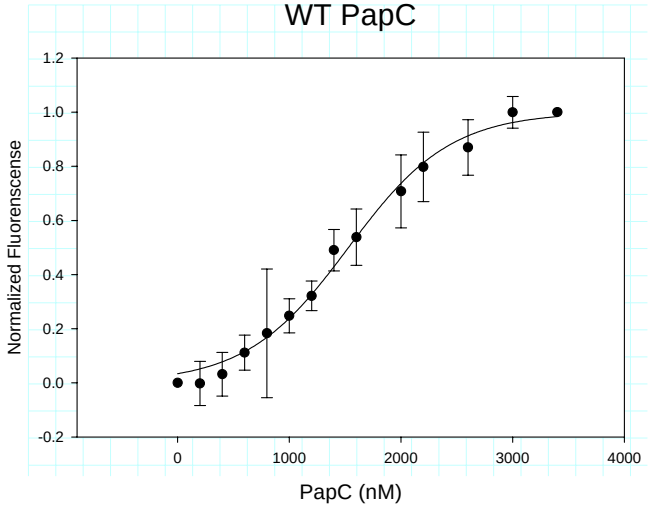
WT PapC
Normalized Fluorenscense
1.2
1.0
0.8
0.6
0.4
0.2
0.0
-0.2
0
1000
2000
3000
4000
PapC (nM)

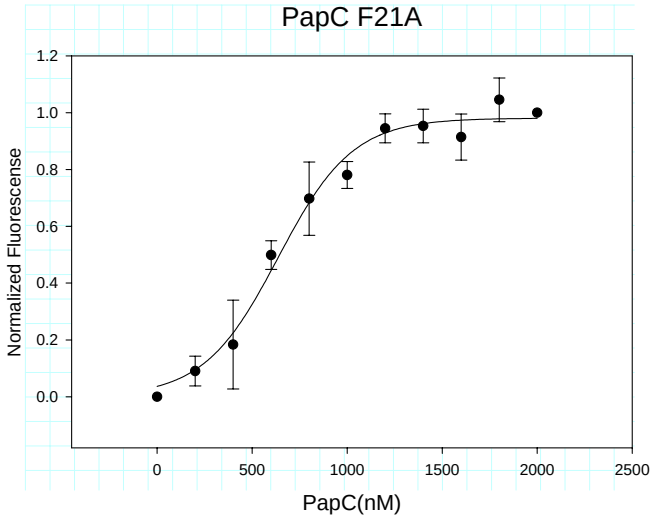
PapC F21A
Normalized Fluorescense
1.2
1.0
0.8
0.6
0.4
0.2
0.0
0
500
1000
1500
2000
2500
PapC(nM)

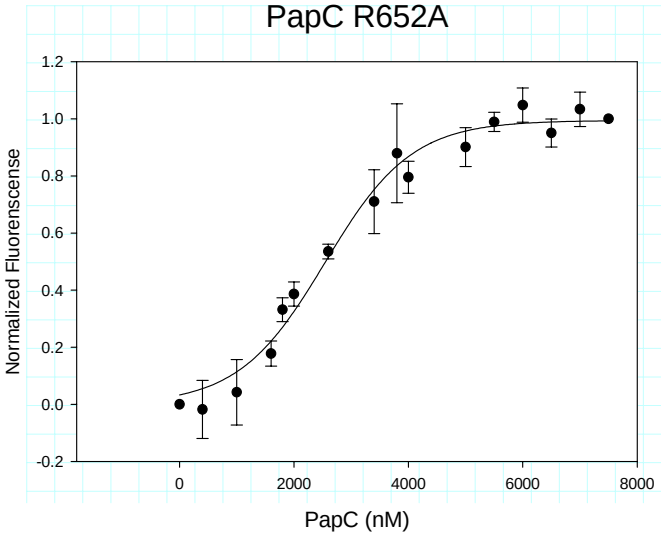
PapC R652A
Normalized Fluorenscense
1.2
1.0
0.8
0.6
0.4
0.2
0.0
-0.2
0
2000
4000
6000
8000
PapC (nM)

Fig. 3-5. PapC-chaperone-subunit binding curves. A. Binding of 25 nM coumarin-labeled PapDG to PapC WT, PapC F21A, PapC R652A. **B.** Binding of 25nM coumarin-labeled $PapDA_{knte}$ to PapC WT, PapC F21A, PapC R652A. X-axis stands for the concentration of PapC usher titrated into PapDG or $PapDA_{knte}$, Y-axis is arbitrary values of normalized fluorescence. The PapC F21A has similar binding affinity to PapDG, and the PapC R652 has decreased binding affinity compared to WT PapC. The PapC F21A has an increased binding affinity to PapDA, and the PapC R652 has slightly increased binding affinity to PapDA compared to WT PapC. Each graph represents average values from at least 3 independent experiments. Error bars represent standard deviation.

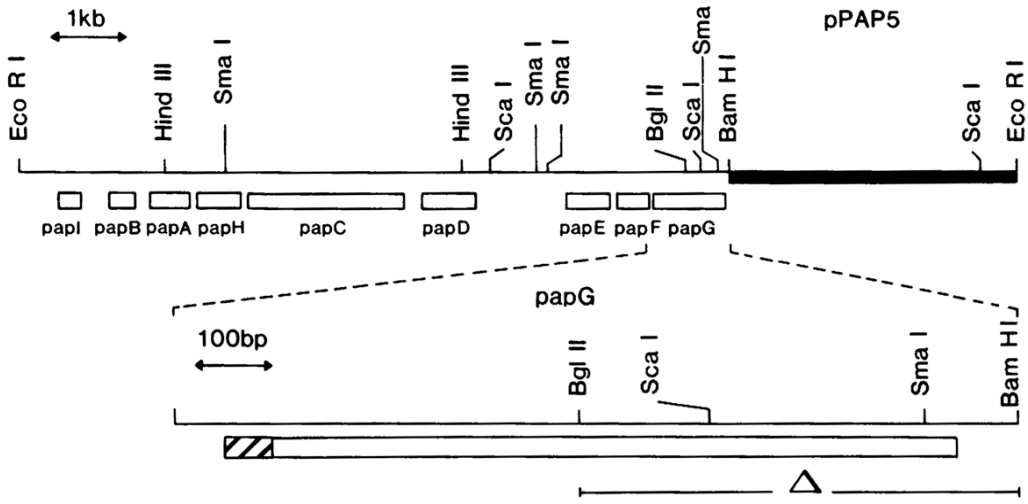

Lund, B. et. al. (1987) Proc. Natl. Acad. Sci. USA 84: 5898-5902.

Fig. 3-6. Restriction map and organization of pPAP5. The location of the *papG* deletion in partial *papG* deletion, pPap24 ('--Δ--') is indicated.

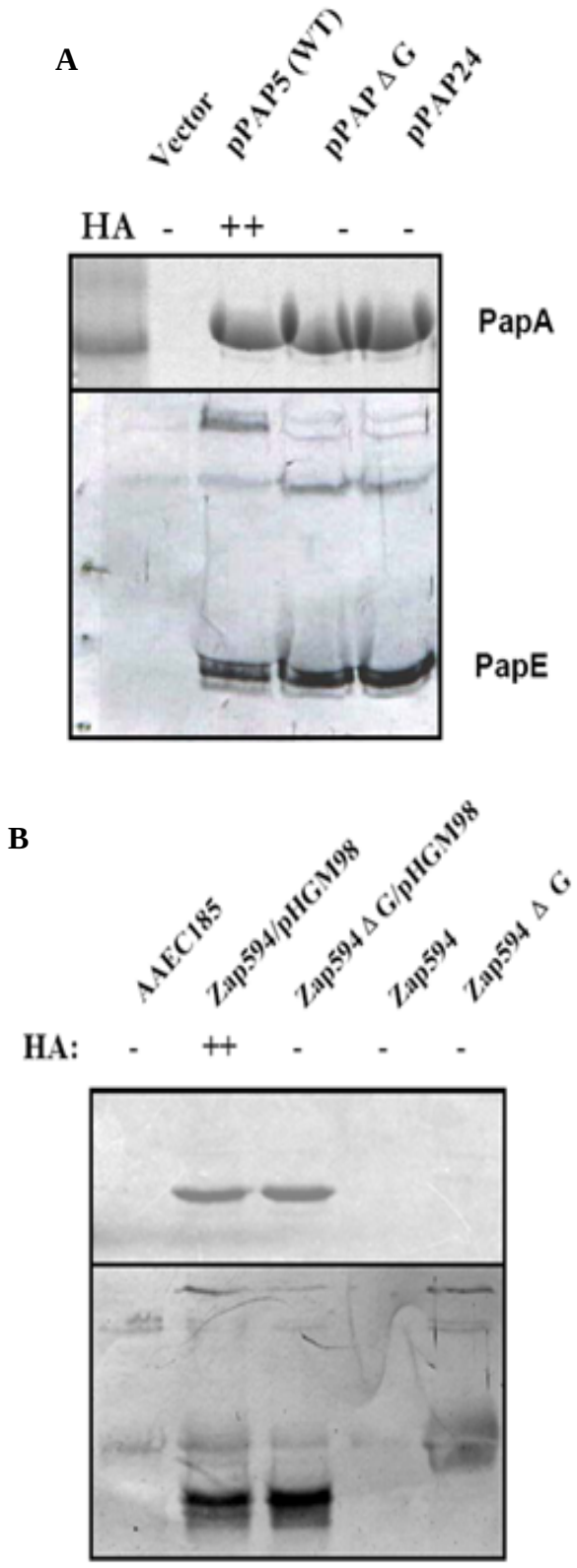

Fig. 3-7. Pilus biogenesis by representative PapG deletion mutants. A. Pili assembled by strain AAEC185 complemented with vector, WT pPap5 or pPapΔG, pPap24 (PapG partial deletion) were examined. **B.** Pili assembled by strain ZAP594, ZAP594ΔG, ZAP594/pHGM98 (*papI*) or ZAP594ΔG/pHGM98 (*papI*) were examined. Pili were isolated from the bacterial surface by heat extraction and magnesium precipitation, and then subjected to SDS-PAGE. The PapA rod subunit was visualized by Coomassie Blue staining (top panel). The PapG and PapE tip fibrillum subunits were detected by immunoblotting with anti-P pilus tip antibody (bottom panel). The qualitative HA for each PapG construct is indicated. (++, strong hemagglutination reaction; -, no agglutination). The pili were isolated from the cell surface of bacteria containing PapG deletion at same level to the WT strains.

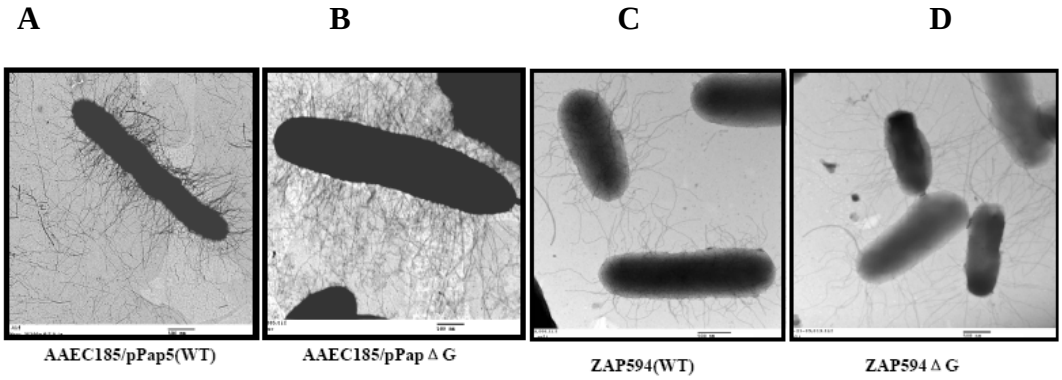

Fig. 3-8. EM analysis of PapG deletion mutants. Pili assembled by strain AAEC185 complemented with wild type pPap5 (A) or pPapΔG (B), or pili assembled by strain ZAP594/pHGM98(*papI*) (C) or *papG* chromosomal deletion strain ZAP594ΔG/pHGM98(*papI*). The bacteria were examined by whole bacteria, negative stain EM. Scar bars represent 500nm. The bacteria harboring *papG* deletion are still able to assemble the pili on the cell surface.

Chapter 4

The Functions of the N- and C-terminal Domains of the PapC usher

Abstract

The crystal structure of the PapC usher showed that the usher contains four distinct domains: a central region containing β-strands that span the OM to form a β-barrel channel, a plug domain which is positioned in the central channel to control the gating, a NTD that is the targeting site for chaperone-subunit complexes, and a CTD that is required for stable chaperone-subunit binding to the usher. To investigate the contribution of the N- and C-terminal domains for channel activity of the PapC usher, I performed antibiotic sensitivity assays using PapC mutants lacking the NTD, CTD or both domains. The results showed that the PapC mutant lacking the NTD or lacking both domains are more sensitive to SDS and antibiotics, which suggests that the NTD plays an important role in PapC channel activity. Previously, a NTD mutant, PapC C70A, was shown to be unable to assemble pili while remaining able to bind to PapDG chaperone-adhesin complexes. To further explore the additional functions of the NTD, overlay and co-purification assays were performed to test the binding ability of PapC C70A to different chaperone-subunit complexes. Our results suggest that PapC C70A is able to bind PapDG and PapDF chaperone-subunit complexes, which ruled out that the defect in pilus assembly of this mutant is due to the defective binding ability to chaperone-subunit complexes.

The PapC usher CTD is required for P pilus assembly and was shown to

stabilize the binding of chaperone-subunit complexes to the usher**.** To further understand the function of the CTD in pilus biogenesis, I performed a functional analysis by mutagenesis study. To narrow down the specific region of the CTD contributing critical roles in pilus biogenesis, a series of C-terminal deletion mutants or alanine substitution mutants were made. The results identified S588-T623 as essential for structural stability, which is consistent with the fact that this region is located within the β-barrel domain from the recently solved crystal structure of the $PapC_{130\text{-}640}$ central region. The other region from PapC G632-R674 was identified as required for pilus assembly. Deletion of a conserved disulfide loop from V791-Q800 on the CTD rendered the PapC usher unstable, which suggested that the conserved disulfide loop also plays a role in PapC structural stability. To screen for functionally important residues within the disulfide loop region, alanine substitution mutants were made and tested for function by hemagglutination assay and pilus isolation. These point mutations only showed slight defects in hemagglutination assay and pilus assembly.

Introduction

Gram-negative bacteria possess a dual membrane envelope that only allows certain molecule to cross. One class of OM proteins, porins, provides channels for exchange of small hydrophilic molecules [139, 140]. The porins have pore sizes of 1.1-1.2 nm in diameter, and the cutoff size of molecules that can diffuse freely is about 550 Daltons [141, 142]. The PapC usher is an integral OM protein and was

demonstrated to be a twin-pore complex, with 2.5 x 4.5 nm diameter channels [100]. A 2.5 nm x 4.5 nm channel is large enough to allow secretion of a linear fiber of folded pilus subunits when the channel is active [25, 143]. Unlike porins, the PapC usher has a plug domain which occludes the volume of the central channel so that non-specific molecules are not able to diffuse across the pore when the PapC channel is inactive. The NTD and CTD of the usher are suggested to locate in periplasm [2]. Our current pilus biogenesis model suggests that the binding of a chaperone-adhesin complex to the NTD or CTD might initiate a conformational change to open the usher channel for pilus secretion [2]. If the NTD or CTD contribute to channel activity, deletion of either or both domains would change the channel activity of PapC. In this study, we analyzed the channel activity of the PapC usher and NTD and CTD deletion mutants using in vivo antibiotic assays.

Pilus biogenesis by UPEC via the CU pathway is a complex process. Pilus assembly on the usher platform involves multiple steps to ensure pilus assembly in the correct order. The NTD of the PapC usher is required for the initial binding of chaperone-subunit complexes, and residues 2-11 are part of the initial binding site. Previously, a PapC C70A mutant was shown to be defective in pilus assembly, while retaining the ability to bind to PapDG chaperone-adhesin complexes. This phenotype could be explained by three possibilities: 1) a defect in binding to chaperone-subunits other than PapDG; 2) a defect in promoting chaperone dissociation from subunit; or 3) a defect in promoting subunit-subunit interaction. In this study, the PapC C70A mutant was further analyzed to explore its binding ability to other chaperone-subunit

complexes in addition to PapDG.

A previous study showed that a PapC CTD truncation mutant lacking A641-K809 correctly targets and folds in the OM [99]. This mutant can bind to PapDG chaperone-adhesin complexes *in vitro* but is unable to complement a *ΔpapC pap* operon to assemble adhesive P pili [118]. Thus, the CTD is required for subsequent events in pilus assembly after the initial targeting of chaperone-subunit complexes to the NTD. However, the detailed mechanism of pilus assembly by the PapC CTD remains unknown. In a previous mutagenesis screening study, several PapC residues were identified, that were shown to be important for the function of the PapC usher. Point mutation of PapC residues C787, C805 and R652 were not able to assemble adhesive P pili and point mutation of PapC residues N673, D701 and E710 were slightly defective in pilus assembly. The previous study also indicated that the conserved C-terminal disulfide loop region plays an important role in pilus biogenesis [118]. To continue screening for functionally and structurally important residues and further narrow down the region of the CTD that is important in pilus biogenesis, additional mutagenesis experiments were conducted.

Results

Deletion of the PapC NTD increases bacterial sensitivity to SDS and Erythromycin. We explored if the NTD and CTD are able to control the central gating system of PapC by using usher truncation mutants lacking these domains. The bacterial OM permeability barrier only allows molecules less than approximately 550

Daltons to cross freely [144, 145], so molecules larger than this cutoff size are normally prevented from entering the bacteria. I used antibiotics larger than 600 Daltons in molecular weight to test channel activity by the usher *in vivo*. Novobiocin (613 Dalton), erythromycin (734 Dalton), rifampicin (823 Dalton) and vancomycin (1449 Dalton) were used in this antibiotics assay. SDS is a long linear chain molecule of 288 Dalton, and it is usually prevented from entering the bacteria by LPS unless the permeability of the bacteria is increased. Therefore, SDS is also included to test the PapC channel activity. The bacteria expressing wild type PapC or truncation mutants lacking the NTD, CTD, or both domains were analyzed for sensitivity to antibiotics and SDS. First, I tested antibiotics sensitivity using a top soft agar diffusion assay. Sensitivity was determined by measuring zones of growth inhibition on agar plates. Bacterial strains expressing different truncation mutants were compared in this assay, which includes the PapCΔ1-128 (ΔN), PapCΔ641-809 (ΔC) and PapCΔ1-128,641-809 (ΔN, ΔC) (Fig. 4-1). The bacterial strain containing wild type PapC usher was used as a positive control and empty vector as a negative control. From this assay, the mutants PapC ΔN and ΔN, ΔC showed more sensitivity to SDS compared to PapC ΔC and wild type (Fig. 4-1). Five repeated experiments showed the same result, which suggested that the NTD may be more important in controlling the channel activity than the CTD. In these top agar assays, significant differences between wild type and mutants to vancomycin, erythromycin, novobiocin or rifampicin were not detected (data not shown). To further investigate the sensitivity of different strains exposed to antibiotics, a CFU assay was performed (Fig. 4-2).

Bacterial cultures expressing vector, wild type PapC, or one of truncation mutants, were grown overnight and diluted into fresh medium. PapC expression was induced with 0.001% arabinose for 30 minutes followed by adding the indicated antibiotics. After growing for 17 hours, the bacterial cultures were serially diluted and plated for colony counting. The mutants PapC ΔN and ΔN, ΔC showed more sensitivity to erythromycin and SDS compared to PapC ΔC and wild type (data not shown). This result suggests that the PapC NTD may contribute more than the CTD to control channel activity, which is also consistent with the data from the top agar assay for SDS sensitivity.

Additional functions of the PapC NTD. Previous studies on PapC mutants C70A and Δ2-11 brought important insights into the function of the NTD in pilus biogenesis [4]. These studies indicated that the 2-11 region of the usher is the initial targeting site for chaperone-subunit complexes. In contrast, PapC C70, which forms part of a conserved N-terminal disulfide loop, is critical for events following the initial targeting of chaperone-subunit complexes. The PapC C70A mutant was unable to complement a Δ*papC pap* operon for P pilus assembly, but remained able to bind PapDG chaperone-adhesin complexes. According to our current pilus biogenesis model (Fig. 1-5), PapDG first targets to the N terminus of the twin-pore usher complex. PapDF targets to the other usher, to allow PapDG and PapDF to form the first link of the pilus fiber. PapC C70A is defective for pilus assembly but has binding affinity for PapDG. The phenotype of this mutant could be caused by loss of binding

affinity for chaperone-subunit complexes other than PapDG, by a defect in promoting subunit-subunit interactions, or by a defect in triggering chaperone release from the subunits. To further define the defect of the PapC C70A mutant, I did *in vitro* overlay and *in vivo* co-purification assays to test binding to individual chaperone-subunit complexes other than PapDG, such as PapDF and PapDK. Overlay assays were performed by isolating OM from bacteria harboring vector alone, wild type PapC, or one of the mutants. Consistent with previous results, PapC C70A strongly bound to PapDG, while no binding was detected between PapCΔ2-11 and PapDG (Fig. 4-3A). Overlay assays testing binding of PapDK or PapDF did not give significant results since only background levels of binding were detected, even with wild type PapC (data not shown). Next, I conducted the co-purification assay to test the usher-chaperone-subunit interactions in vivo. OM was isolated from bacteria co-expressing PapDG, PapDF or PapDK with the WT PapC or PapC C70A mutant. The samples were then passed over a nickel affinity column to test if the chaperone-subunit complexes were pulled down with the PapC usher. The results from the co-purification assays showed that PapC C70A was able to bind PapDF in addition to PapDG (Fig. 4-3B). To confirm that this result was not due to different expression levels of the chaperone-subunit complexes by the different strains, I checked the expression level of PapDG and PapDF in whole bacteria harboring mutant or wild type PapC, and found the chaperone-subunit complexes were expressed similarly in all strains (data not shown). Finally, using the established fluorescence-based assay, I tested the binding affinity of PapC C70A to PapDG and

the titration curves showed an apparent dissociation constant of 62 $\pm$ 6 nM, which is similar to the PapC wild type (Fig. 4-4 and Fig. 3-5 A). These results confirmed that the PapC C70A can bind to the PapDG and has the similar binding affinity compared to the PapC wild type. All these results support that the NTD mutant PapC C70A is able to bind not only PapDG but PapDF as well, suggesting that the assembly defect must occur at a subsequent step of pilus assembly such as catalyzing the exchange of chaperone-subunit for subunit-subunit interactions.

The Contribution of PapC S588-T623 and PapC G632-R674 to overall folding of the PapC usher. To investigate regions of the CTD that are important for PapC structure and pilus assembly, we constructed several PapC deletion mutants. I checked the expression and proper folding of these mutants in whole bacteria and OM preparations before functional analysis. The expression of each mutant showed similar or slightly reduced levels compared to the wild type PapC, by running equivalent amounts of whole bacteria in SDS-PAGE and immunoblotting with anti-usher antibody (data not shown). We next took advantage of the β-barrel structure of PapC to check the proper folding of the mutants. OM β-barrel proteins are resistant to SDS denaturation at low temperature, so the compact folded proteins migrate faster in SDS-PAGE compared to the linear denatured proteins and show a heat-modifiable mobility shift [97]. From the heat modifiable mobility assay, I found that the truncation mutants PapCΔ588-623, Δ588-599, Δ600-609 and Δ610-619 lost heat modifiable mobility on SDS-PAGE (Fig. 4-4). In contrast, the deletion mutants

PapCΔ632-764, Δ640-649, Δ650-659 and Δ660-669 showed heat modifiable mobility similar to wild type PapC (Fig. 4-4), suggesting that these regions in the CTD of the PapC usher does not affect overall folding of the usher.

PapC G632-R674 is required for P pilus assembly. To further investigate the *in vivo* function of the PapC deletion mutants, I tested the ability of the mutants to complement a plasmid carrying a *ΔpapC pap* operon, to form pili. Hemagglutination assays (HA) were conducted to test the presence of adhesive pili on the bacterial surface. The wild type PapC gave an HA titer of 128 while the vector control gave a titer of zero. All the PapC deletion mutants Δ588-623, Δ588-599, Δ600-609, Δ610-619, Δ632-764, Δ640-649, Δ650-659 and Δ660-669 were defective in causing agglutination of human blood cells with HA titer of 0 to 4 compared to wild type 128 (Fig. 4-6 and Table 4-1). The HA assays were confirmed by purification of pili from these mutants. Consistent with the HA assay, all the PapC deletion mutants showed defects in pilus assembly (Fig. 4-6). The loss of function of the PapC deletion mutants in PapC S588-T623 is likely due to the fact that this region is important for proper folding of PapC. The deletion mutants in the region of PapC G632-R674 were not shown to change the overall folding of the usher, but lost the function to assemble P pili, demonstrating that PapC G632-R674 is required for pilus assembly. This phenotype is also consistent with previous data from the alanine substitution mutant PapC R652A in the same region [118], which signifies the importance of this region of the CTD in pilus biogenesis.

The conserved disulfide loop is structurally important for the PapC usher. The PapC C terminus contains a conserved pair of cysteine residues C787 and C805, and C787 was previously shown to be critical for pilus assembly [118]. The CTD disulfide loop is conserved in the usher superfamily. I analyzed the function of residues within the C-terminal disulfide loop region. Charged and polar residues within the disulfide loop were previously mutated to alanine, but did not cause a detectable pilus assembly phenotype (S. So, unpublished data). To continue the previous mutagenesis screening study, I substituted alanine for the remaining 10 amino acids within this loop region. Examination of the expression of these mutants showed similar levels compared to the wild type PapC, and all of the alanine substitution mutants folded properly. HA assay showed only a slightly defective HA titer of 64 for all the mutants compared to the wild type PapC HA titer of 128 (Fig. 4-6). The HA results were confirmed by pilus purification analysis (Fig. 4-6 and Table 4-1). I also made a deletion of V791-Q800 within the disulfide loop. Examination of its expression level and heat mobility shift showed that this deletion mutant was not stable or folded properly (data not shown), suggesting that the disulfide loop is critical to keep proper folding of the usher. HA titer of the mutant was 0 compared to wild type with a HA titer of 128, and pilus extraction showed no pilus formation. Thus, mutation of the individual residues in the disulfide loop did not significantly affect the function of PapC in pilus assembly, but the disulfide loop region appears to play a critical role in proper structure of the usher.

The PapC CTD contributes to the binding of chaperone-tip subunits to the usher.

The first step in pilus assembly is the targeting of chaperone-subunit complexes to the usher NTD. As shown previously, some of the PapC CTD mutants are defective in assembling adhesive pili on the cell surface (Fig.1-5). To further identify which specific assembly step is affected in these mutants, I performed a co-purification assay of the PapC deletion mutants with chaperone-tip subunits. OM was isolated from strain SF100 harboring pPAP58 (PapDJEFG) together with vector, WT PapC or the indicated PapC mutants. The OM was solublized with DDM and then passed through a HisTrap column. As shown in Table 4-2, all the mutants were not able to interact with chaperone-tip subunits complexes and gave the HA titer as 0 except PapCΔ588-599 compared to wild type 256 (Table 4-3). The results from this co-purification assay suggests that the indicated PapC mutants are defective in pilus assembly due to a defect in stable binding to the chaperone-tip subunit complexes, similar to the phenotype of a PapCΔ640 mutant [118]. Previous data showed that PapC R652A was defective in pilus biogenesis, but is able to bind to pilus tips. It suggests that PapC R652 might be only available to contribute the stable binding following the initial binding of PapDG to the NTD. The rest of residues within G623-R674 region might be still involved in binding of chaperone-tip complexes.

Discussion

The recent crystal structure of PapC demonstrated that the usher has four distinct domains: central β-barrel domain; plug domain; NTD and CTD [2]. The plug domain locates in the middle of the β-barrel region and occludes the central pore of

the usher [2]. The CTD is thought to be positioned partially under the PapC channel and might directly contact with plug domain [2, 101]. The central channel is 4.5 x 2.5 nm in diameter, which is enough for folded pilus subunit to go through. The antibiotics assay data presented here showed that deletion of the NTD affects the channel activity, indicating that the NTD is involved in the PapC gating system. This *in vivo* study did not support that the CTD affects the channel activity, but more studies are needed to determine the direct roles of each domain in channel gating. Recent experiments by our collaborators were performed using *in vitro* planar lipid bilayer electrophysiology to characterize the channel activity of wild type PapC and PapC mutants deleted for both the NTD and CTD. The results showed that small channel openings are present most of the time in the mutant lacking both NTD and CTD compared to wild type PapC, although these channels do not represent complete opening of the plug [128]. These small channels may be sufficient for entry of small molecules such as SDS and erythromycin.

A previous mutagenesis study identified the PapC C70A mutation in the conserved disulfide loop as defective for P pilus formation, while overlay and co-purification assays indicated that this mutant was able to bind to PapDG chaperone-adhesin complexes [4]. In agreement with this, the PapC C90A and Δ77-85 mutants, which also have mutations in the conserved disulfide loop of the N terminus, had identical phenotypes (T. Ng., unpublished data). In this study, overlay experiments were repeated and resulted in the same phenotype. Furthermore, the PapC C70A mutant co-purified not only with PapDG but PapDF as well, which

indicated that the C70A mutant is not defective in recruitment of different chaperone-subunit complexes. This data suggests that PapC C70A must be defective for catalyzing the formation of subunit-subunit interactions. In agreement with this, a previous experiment took advantage of the fact that subunit-subunit interactions in the pilus fiber are stable to SDS unless heated above 65ºC [146]. The pilus subunits that co-purified with the usher were treated at 25ºC or 95ºC in SDS sample buffer and examined for stable subunit-subunit interactions by SDS-PAGE and immunoblotting with anti-PapDG antibodies. For the WT PapC sample treated at 25ºC, the monomeric PapG band disappeared and PapG was clearly assembled into an oligomeric structure. In contrast, for PapC C70A mutant, the monomeric PapG band remained and no oligomeric structure was apparent. The loss of subunit-subunit oligomerization suggested that PapC C70A is defective in promoting assembly of the adhesin into a pilus fiber. Combined with current experiments and previous data, the N-terminal cysteine loop appears to be critical for the catalytic activity of the usher in promoting subunit-subunit interactions during pilus biogenesis.

The CTD is required for stages of pilus biogenesis following the initial targeting of chaperone-subunit complexes to the NTD [118]. The last 169 residues of PapC (following PapC A640) are not required for overall folding of the usher [99], which is confirmed by the recently solved crystal structure of the PapC central β-barrel region showing that the CTD is a separate domain from the central β-barrel region [2]. In the current study, PapC deletion mutants within S588-T623 rendered the PapC usher structurally unstable. The phenotypes of these mutants are consistent

with the fact that PapC usher S588-T623 is a part of the central β-barrel domain by recently solved crystal structure (Fig. 1-3) [2]. Here the G632-R674 region is identified to be required for pilus biogenesis but not the structural stability for the usher. This is in agreement with the phenotype of the PapCΔ640 CTD deletion mutant, which is non-functional in pilus biogenesis. Our co-purification assay showed that the deletion mutants within G632-R674 are not able to form stable complexes with the chaperone-tip subunits *in vivo.* This phenotype is also similar to the PapC Δ640, which also was unable to co-purify with chaperone-subunit complexes [118].

Although the PapC deletion mutant lacking the whole CTD did not affect the overall structure of PapC, our deletion mutant lacking just the CTD disulfide loop region affected the structure of the usher. It is possible that the smaller deletion causes the local structure of the CTD to be altered and this affects the overall structure of the PapC main core.

In summary, the functions of the CTD of PapC are involved in: 1) Stable binding to chaperone-subunit complexes after initial targeting of chaperone-subunit complexes to the NTD; 2) PapC overall structural stability; 3) high affinity binding to chaperone-adhesion complexes.

Table 4-1. Hemagglutination Assay, Pilus Assembly and Heat Mobility of PapC Deletion Mutants.

Strains	HA titer	Pilus assembly	Heat modifiable mobility
vector	0	None	None
PapC (WT)	128	WT	WT
PapC Δ588-623	0	Defective	None
PapC Δ588-599	4	Slight assembly	None
PapC Δ600-609	0	Defective	None
PapC Δ610-619	0	Defective	None
PapC Δ632-674	0	Defective	same as WT
PapC Δ640-649	0	Defective	same as WT
PapC Δ650-659	0	Defective	same as WT
PapC Δ660-669	0	Defective	same as WT
PapC Δ791-800	0	Defective	None

Table 4-2. Co-purification assay with pilus tips.

Strains	[a]Co-purification
SF100/Pap58/pMON	-
SF100/Pap58/papC640Δ	-
SF100/Pap58/pMJ3	+
SF100/Pap58/PapCΔ588-623	-
SF100/Pap58/PapCΔ588-599	-
SF100/Pap58/PapCΔ600-609	-
SF100/Pap58/PapCΔ610-619	-
SF100/Pap58/PapCΔ632-674	-
SF100/Pap58/PapCΔ640-649	-
SF100/Pap58/PapCΔ650-659	-
SF100/Pap58/PapCΔ660-669	-

[a]Co-purification: "+" stands for chaperone-tip subunit complexes were co-purifed with the PapC usher
"-"stands for chaperone-tip subunit complexes were unable co-purified with the PapC usher.

Table 4-3. Hemagglutination Assay with pilus tips.

Strains	[a]HA titer
SF100/Pap58/pMON	0
SF100/Pap58/PapC640Δ	0
SF100/Pap58/pMJ3	256
SF100/Pap58/PapCΔ588-623	0
SF100/Pap58/PapCΔ588-599	4
SF100/Pap58/PapCΔ600-609	0
SF100/Pap58/PapCΔ610-619	0
SF100/Pap58/PapCΔ632-674	0
SF100/Pap58/PapCΔ640-649	0
SF100/Pap58/PapCΔ650-659	0
SF100/Pap58/PapCΔ660-669	0

[a]HA titer is the highest fold dilution of bacteria able to agglutinate human red blood cells.

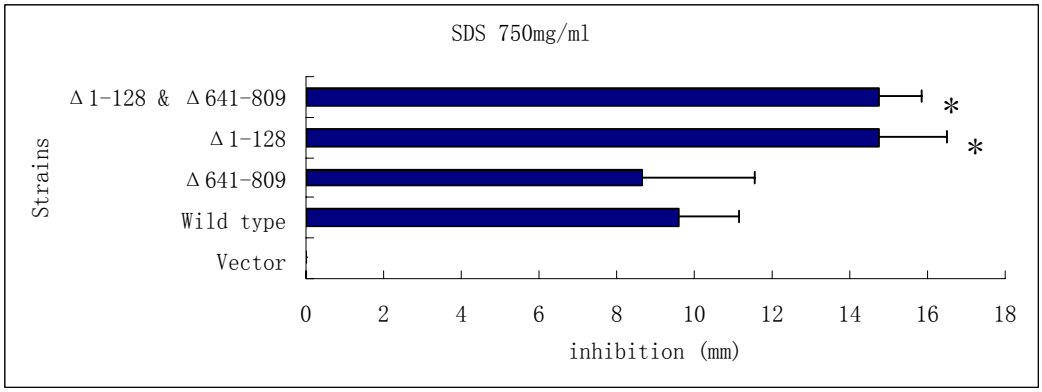

Fig. 4-1. Sensitivity of the PapC deletion mutants to SDS. Bacteria harboring vector, wild-type PapC or the PapC truncation mutants were exposed to 6 mm diameter discs pre-soaked with 10 μl 750 mg/ml SDS. The diagram represents the average of five independent assays, which measured the diameter of the zone of inhibition minus the disc diameter (6 mm). * Represents p value, which is calculated with t-test. $p < 0.01$.

A

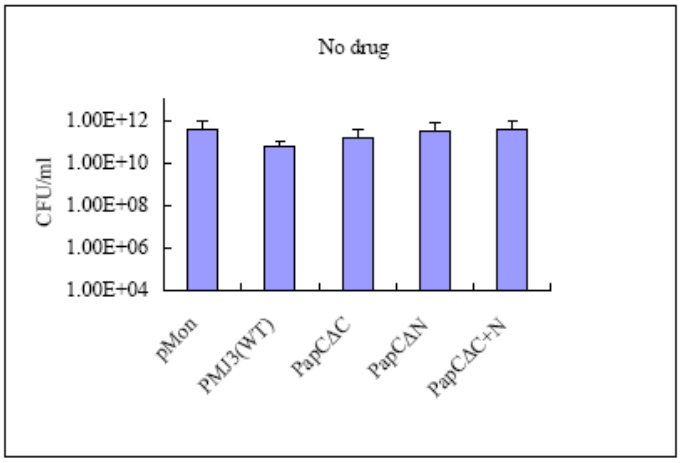
No drug
CFU/ml
1.00E+12
1.00E+10
1.00E+08
1.00E+06
1.00E+04
pMon
PMJ3(WT)
PapCΔC
PapCΔN
PapCΔC+N

B

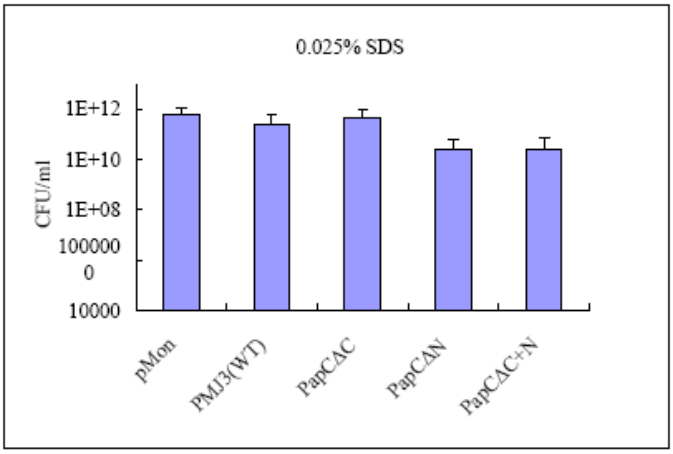
0.025% SDS
CFU/ml
1E+12
1E+10
1E+08
100000
0
10000
pMon
PMJ3(WT)
PapCΔC
PapCΔN
PapCΔC+N

C

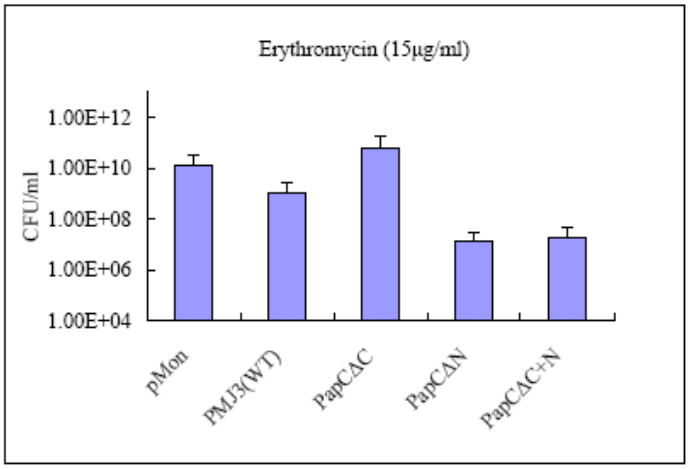
Erythromycin (15μg/ml)
CFU/ml
1.00E+12
1.00E+10
1.00E+08
1.00E+06
1.00E+04
pMon
PMJ3(WT)
PapCΔC
PapCΔN
PapCΔC+N

D

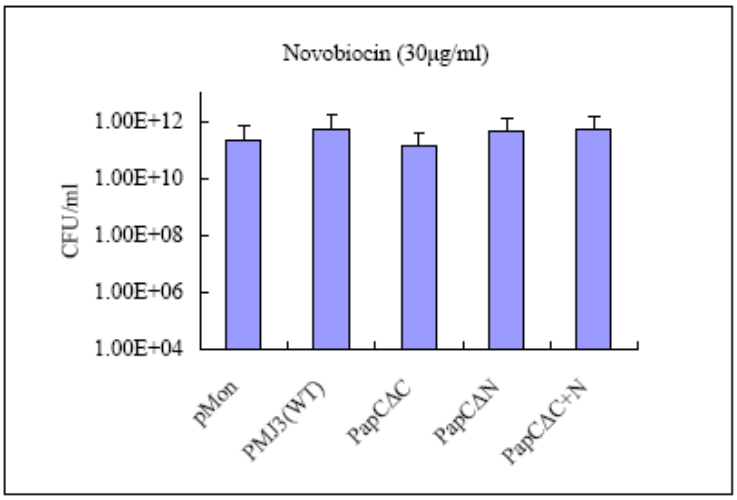
Novobiocin (30μg/ml)
CFU/ml
1.00E+12
1.00E+10
1.00E+08
1.00E+06
1.00E+04
pMon
PMJ3(WT)
PapCΔC
PapCΔN
PapCΔC+N

E

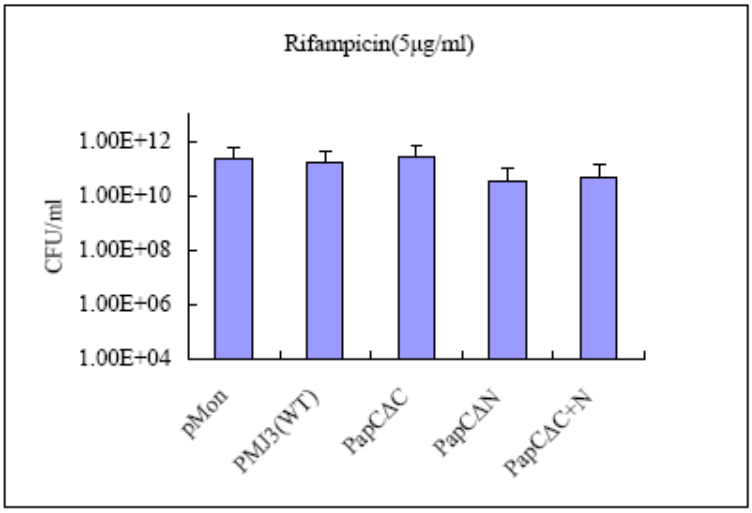
Rifampicin(5μg/ml)
CFU/ml
1.00E+12
1.00E+10
1.00E+08
1.00E+06
1.00E+04
pMon
PMJ3(WT)
PapCΔC
PapCΔN
PapCΔC+N

F

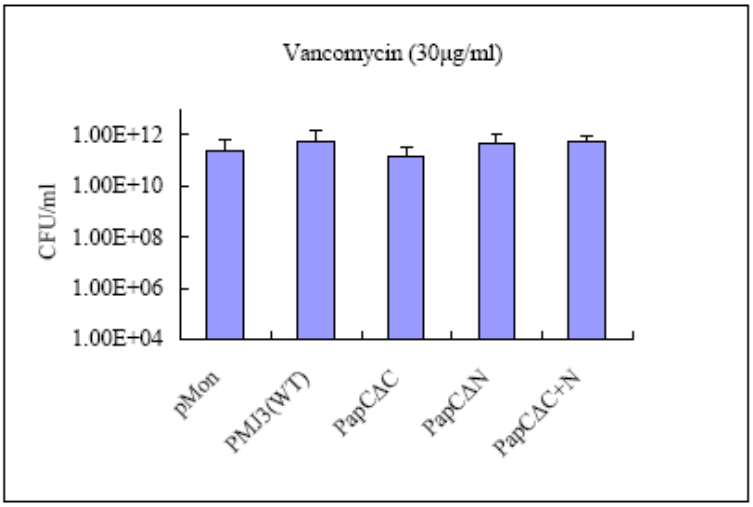
Vancomycin (30μg/ml)
CFU/ml
1.00E+12
1.00E+10
1.00E+08
1.00E+06
1.00E+04
pMon
PMJ3(WT)
PapCΔC
PapCΔN
PapCΔC+N

Fig. 4-2. Sensitivity of the PapC truncation mutants to various antibiotics. Bacteria harboring pMON (vector), wild-type PapC or the PapC truncation mutants were grown in the presence of the indicated antibiotics for 17 h and then plated to determine CFU. (A) No drug; (B) 0.025% SDS; (C)15 μg/ml erythromycin (D) 30 μg/ml novobiocin; (E) 5 μg/ml rifampicin; (F) 30μg/ml vancomycin for 17 hours, serially diluted and plated on the agar plates at 37℃ overnight. Results shown are the averages from three independent experiments. Error bars represent standard deviations.

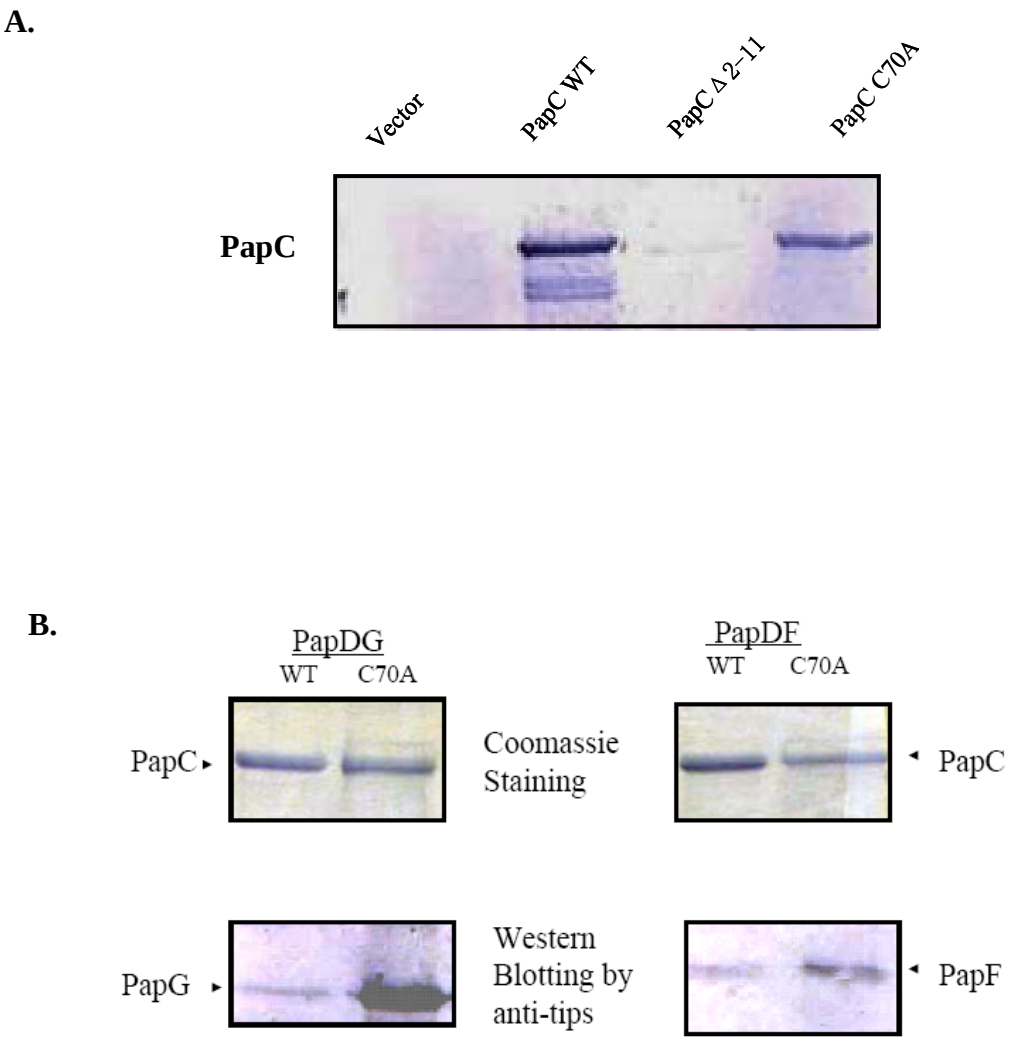

Fig. 4-3. PapC-chaperone-subunit interaction. (A) Overlay assay for binding of PapDG chaperone-adhesin complexes to PapC. OM was isolated from SF100 expressing the vector alone, WT PapC, PapC Δ2-11, or PapC C70A. Samples were separated by SDS-PAGE and transferred to PVDF membrane for the overlay assay. **(B)** Co-purification of P pilus tip subunits with the PapC usher. OM was isolated from strain SF100/pJP (*papDG*) or SF/pMJ4 (*papDF*) expressing the WT PapC or PapC C70A. OM was solubilized with DDM and PapC was purified by nickel affinity chromatography. The eluted fractions were subjected to SDS-PAGE and stained with Coomassie blue to detect purified PapC (upper panel), or immunoblotted with anti-P pilus tip antibody (bottom panel). The PapC C70A is able to bind PapDG and PapDF *in vivo*.

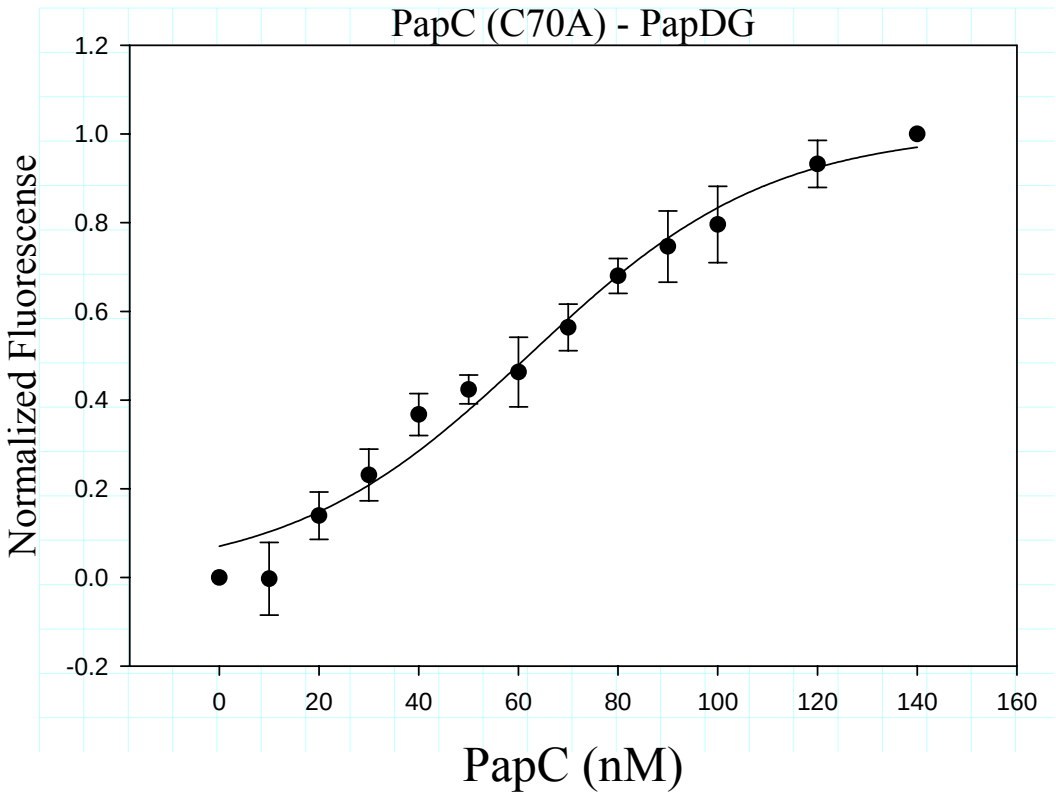

Fig. 4-4. Binding of 25 nM coumarin-labeled PapDG to PapC C70A. X-axis indicates the concentration of PapC C70A usher titrated into PapDG, Y-axis is arbitrary values of normalized fluorescence. The PapC C70A has similar binding affinity to PapDG, compared to WT PapC.The graph represents average values from 5 independent experiments. Error bars represent standard deviation. The apparent Kd value of PapC C70A to PapDG is 62 $\pm$ 6 nM.

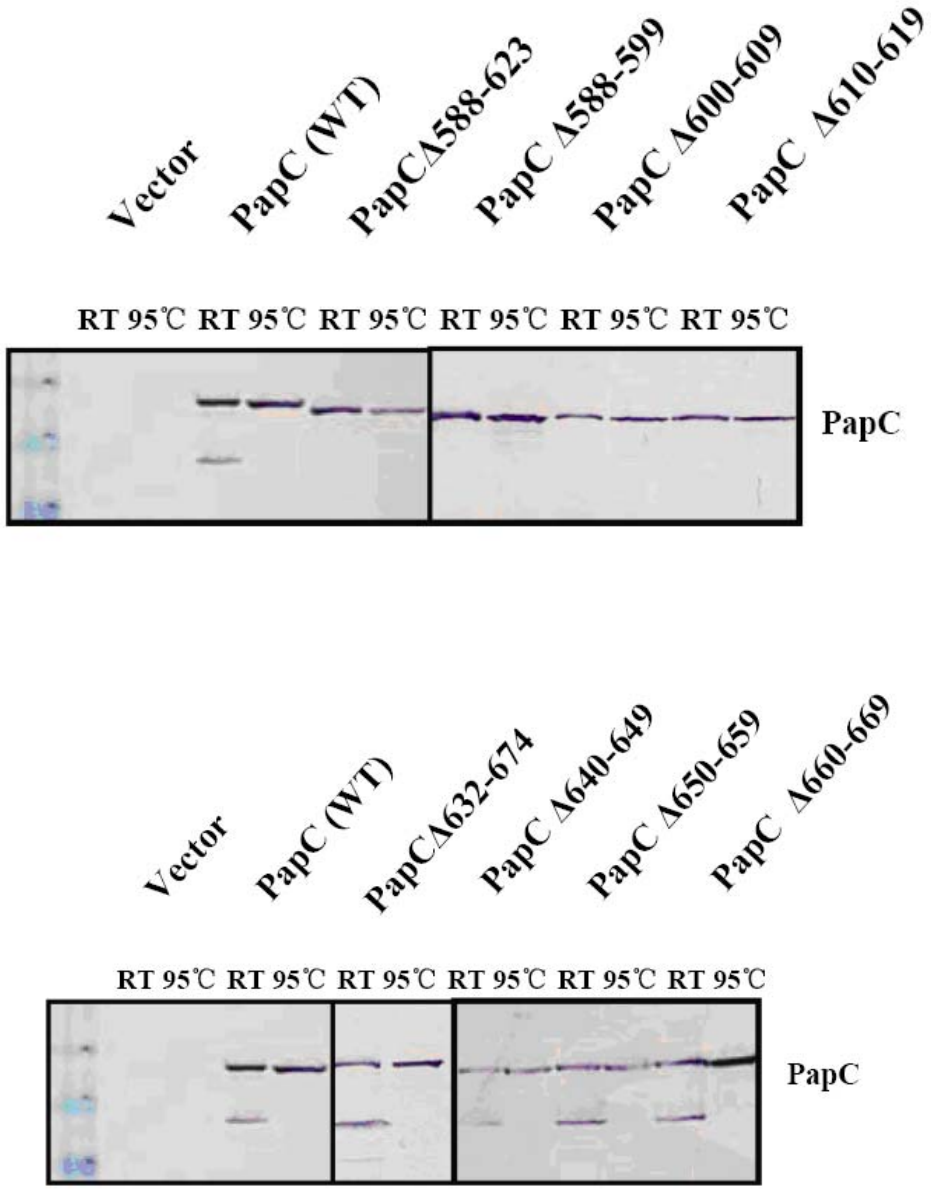

Fig. 4-5. Expression and folding of PapC CTD mutants. OM was isolated from SF100 expressing WT PapC or the indicated PapC mutants and incubated for 10 min in SDS sample buffer at room temperature or 95℃ prior to separation by SDS-PAGE. The ushers were detected by immunoblotting with anti-his antibody. The WT usher exhibit heat-modifiable mobility, indicating proper folding in the OM. The CTD deletion mutants within S588-T623 affect the overall folding of the PapC whereas the mutants within G632-R674 are able to fold correctly.

A

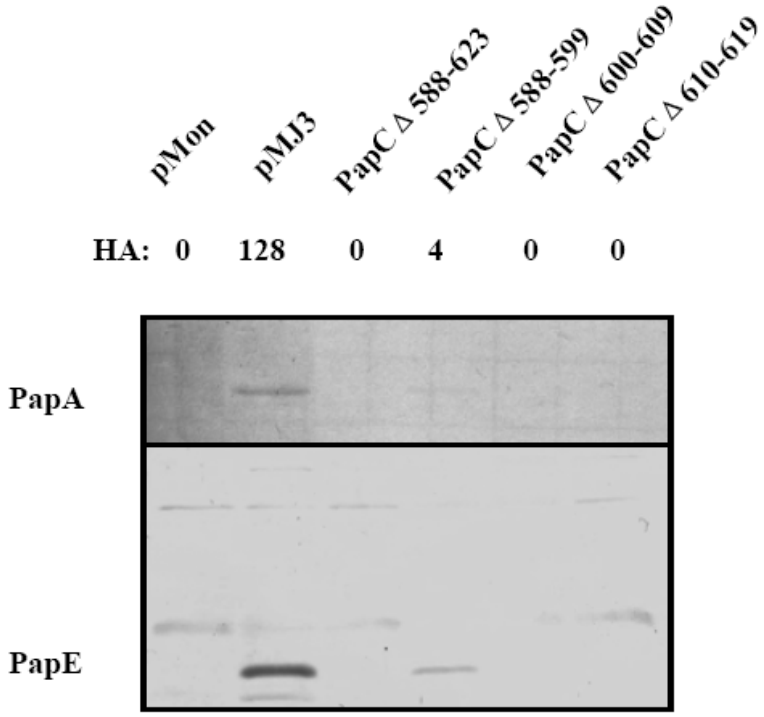
pMon
pMJ3
PapC Δ 588-623
PapC Δ 588-599
PapC Δ 600-609
PapC Δ 610-619
HA: 0 128 0 4 0 0
PapA
PapE

B

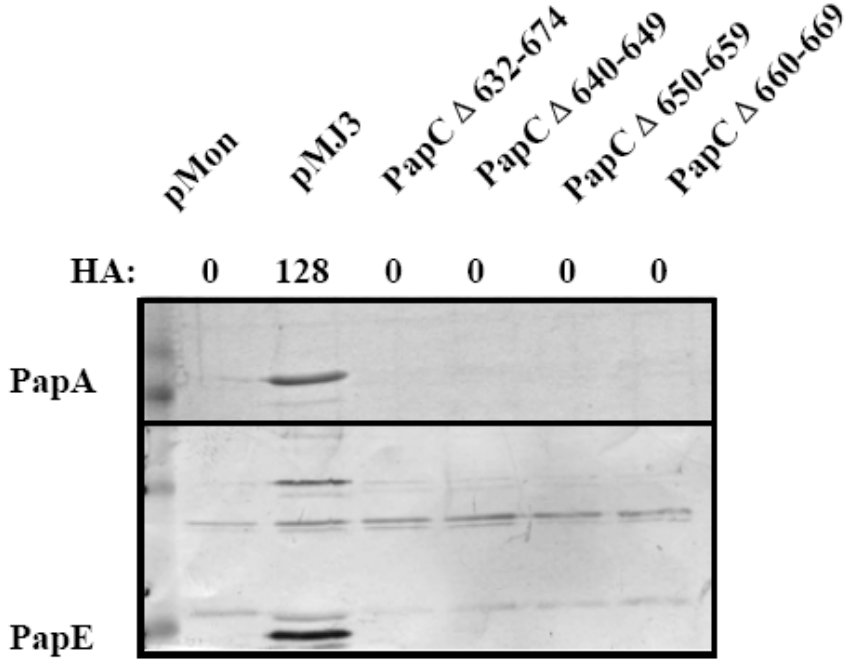
pMon
pMJ3
PapC Δ 632-674
PapC Δ 640-649
PapC Δ 650-659
PapC Δ 660-669
HA: 0 128 0 0 0 0
PapA
PapE

C

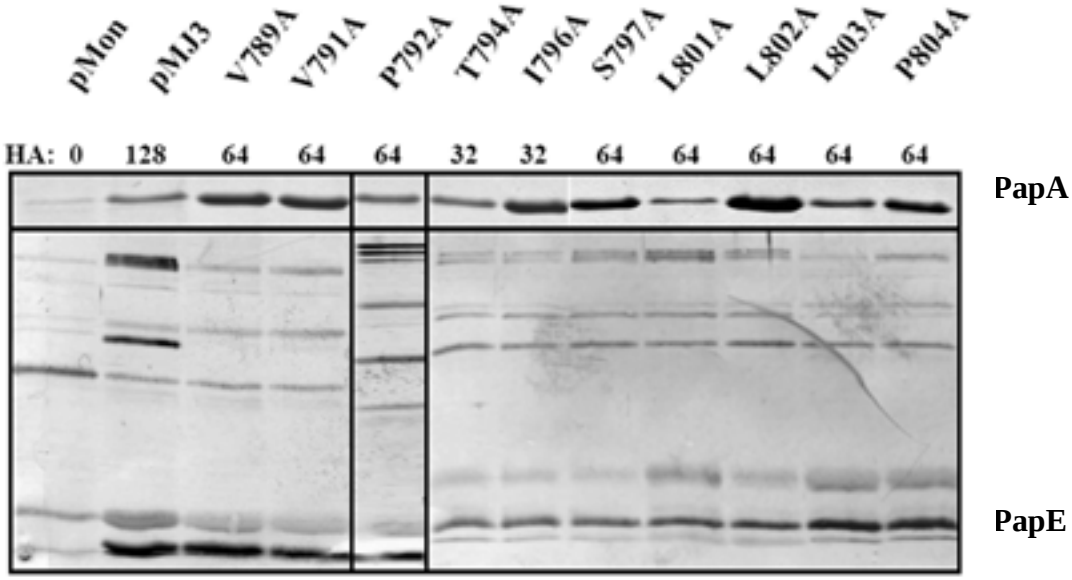

Fig. 4-6. P pilus assembly by representative PapC CTD mutants. Strain AAEC185/pMJ2() was complemented with vector only, WT PapC or the indicated PapC mutant. Pili were isolated from the bacterial surface by heat extraction and magnesium precipitation, and then subjected to SDS-PAGE. The PapA rod subunit was visualized by Coomassie Blue staining (upper panel). The PapE subunits were detected by immunoblotting with anti-P pilus tip antibody (lower panel). The HA titer for each PapC is indicated. A) 588-623 region; B) 632-674 region; C) Point mutations in CTD disulfide loop. The deletion mutations within 588-623 region cause PapC to be unstable in overall folding and defective in pilus biogenesis; the deletion mutations within 632-674 are non-functional for pilus biogenesis; the point mutations within disulfide loop have slight defects in pilus biogenesis.

Chapter 5

Conclusions and Future Directions

Conclusions:

The experimental data from my dissertation has provided insights into molecular interactions during pilus biogenesis by the PapC usher and the functions of the PapC N- and C-terminal domains. The NTD and CTD are proposed as two globular soluble domains located in the periplasm [2, 101]. The X-ray structure of the NTD of FimD was solved previously and shown to form a soluble, globular domain (Fig. 1-4) [101]. In this study, I developed an *in vitro* fluorescence technique that allowed us to measure protein-protein interactions involved in the process of pilus biogenesis. Previous experiments identified PapC F21A and R652A as defective in pilus assembly but able to form functional tip fibrillae in the absence of the PapA rod subunit. We hypothesized that these two mutants were defective in recognition of chaperone-subunit complexes during the process of pilus assembly. We measured protein interactions between the PapC alanine substitution mutants and chaperone-subunit complexes and identified that PapC F21A has higher binding affinity to PapDA but similar affinity to PapDG compared to wild type PapC. In contrast, PapC R652A has dramatically decreased binding affinity to PapDG and 2-fold lower affinity to PapDA complexes compared to wild type PapC. This suggests that the NTD residue F21A is more likely involved in controlling affinity to PapDA. In the presence of much higher concentration of PapDA in the periplasm, PapDG is

outcompeted for binding to the PapC F21A mutant by PapDA. In contrast, PapC R652 seems more likely involved in high affinity binding to PapDG after initial binding of PapDG to the NTD. The binding affinity to PapDG is dramatically decreased in the PapC R652A mutant compared to the change in binding to PapDA. The different phenotypes of the mutants in NTD and CTD emphasizes the different roles of these domains, which suggests that the NTD might be more important for discrimination among chaperone-subunit complexes whereas the CTD might be more important for high affinity binding to PapDG.

The PapC usher forms dimeric complexes with a channel in each monomer [100]. The size of each channel is 4.5 x 2.5 nM in diameter which is two fold bigger than the size of porins. Pilus biogenesis is a process of protein secretion across the IM, periplasm and OM, and the channel opening of the usher is a key step in pilus assembly. In this dissertation, I presented results from an antibiotics sensitivity assay, which investigated the function of the NTD and CTD in controlling channel activity. My results showed that PapC mutants lacking the NTD were more sensitive to SDS and erythromycin, which suggested that the NTD plays an important role in channel activity. According to our current model of P pilus biogenesis (Fig. 1-5), after recruitment of chaperone-subunit complexes from the periplasm, the usher must undergo a conformational change and the plug domain must rotate to accommodate the subunit to cross through the central channel. Here, the PapC mutant deletion of both N- and C-terminal domains showed altered channel activity while the plug domain is still in place. This phenomenon could be due to the N- and C-terminal

domains affecting the location of the plug domain or directly contacting the plug domain in the process of pilus assembly so that the size of the channel could be changed. Another possibility is that N- and C-terminal domains might transiently replace the plug domain during pilus assembly. Previous cryon-EM data suggested that the CTD might be located underneath the PapC channel and be more important for controlling the channel opening [102]. The data from my antibiotics assays suggests that the NTD is more critical for the channel activity. The difference between the EM data and my data could be explained by the fact that the CTD might directly contact the plug domain and the NTD might directly contact the CTD and ensure the proper position of the CTD. Upon deletion of the NTD, the CTD could be no longer able to contact the plug domain or its position maybe be altered, resulting in the leaking of the channel. In our antibiotics assays, the mutant lacking the CTD was not sensitive to the SDS or antibiotics. One possible explanation is that the NTD might replace the position of the CTD to secure the plug and prevent the leaking of the channel.

Previous functional analysis suggested that PapC C70 is involved in promoting subunit-subunit interactions. The further functional analysis of the PapC70A presented in this dissertation showed that this mutant is able to bind to chaperone-subunit complexes in addition to PapDG, which excludes the possibility that the loss of function of pilus assembly is due to defects in binding to chaperone-subunit complexes.

Thus, the N-terminal domain has been shown to be critical and has the

versatile functions in P pilus biogenesis: 1) the initial targeting site of chaperone-subunit complex; 2) confers specificity to the usher; 3) controlling channel activity of usher; 4) promoting subunit-subunit interactions; 5) discriminating between different chaperone-subunit complexes.

Analysis of PapC deletion mutants revealed that the region G632-R674 is required for pilus assembly although deletion of this region did not affect the overall folding of the PapC usher. Furthermore, co-purification analysis indicated that the deletion mutants in this region are defective in binding to chaperone-tip subunit complexes. The previously identified PapC mutant R652A was shown to be required in pilus biogenesis but able to co-purify with chaperone-tip subunits. My results show that PapC R652 is important for high affinity binding to the chaperone-adhesin and might be available after initial chaperone-subunit recruitment to the NTD. Loss of other residues within the G632-R674 region could result in a defect in overall binding to the chaperone-tip complexes, so that the deletions cause a loss of stable binding to the chaperone-tip complexes [118]. PapC C-terminal alanine substitution mutants within the conserved disulfide loop only showed slight defects in pilus assembly, whereas a 10 amino acid deletion within the disulfide loop caused PapC to not fold correctly. Unlike the disulfide loop within the NTD, the C-terminal disulfide loop is required for stabilization of the structure of the PapC usher. Thus, this signifies different roles of the NTD and the CTD: NTD is functionally required whereas the CTD is more structurally required in pilus biogenesis.

The PapG adhesin is located at the distal end of the P pilus (Fig. 1-1), and is

required for recognition and colonization of the host cell. PapG is responsible for the virulence and specificity of the bacteria. In our current model for pilus biogenesis (Fig. 1-4), binding of the chaperone-adhesin complex to the usher is required for pilus biogenesis. In type 1 pili, the adhesin FimH is an initiator and triggers a conformational change upon targeting to the FimD usher [119]. However, in this study, I found that deletion of PapG did not affect P pilus assembly, which shows that PapG is not the initiator of P pilus assembly. Previously, PapF and PapK were reported as initiators for P pilus assembly [136]. Thus, the correct affinity of PapDG chaperone-adhesin complexes to PapC usher is likely a key step to ensure that PapG is the first subunit to be incorporated into a pilus fiber. In the absence of PapG, pili still assemble on the bacterial surface, but these pili would be non-functional in colonization.

In summary, this study presented new information on the roles of the NTD and CTD in pilus biogenesis. According to the recently solved crystal structure of PapC, EM data, previous functional analyses of PapC, and current quantitative ananlysis of usher-chaperone-subunit interactions, the NTD and CTD are involved in pilus biogenesis including every step in chaperone-subunit recruitment, assembly and secretion. Our model of pilus biogenesis indicates that chaperone-subunit complexes are recruited in order by specific affinity to the usher; the NTD is the initial targeting site and the CTD stabilizes the binding of chaperone-subunit complexes in a subsequent stage. In this study, analysis of PapC F21, R652, C70A and regions with G632-R674 and V791-Q800 on NTD and CTD signified the important functions of

both domains in pilus biogenesis.

Future Directions

In vitro analysis of protein-protein interactions involved in pilus biogenesis. The periplasmic chaperone keeps pilus subunits in a high-energy conformation, but in the absence of the usher the transition from chaperone-subunit complexes to subunit-subunit interactions is very slow [114]. Therefore, we hypothesize that the usher acts as a catalyst to trigger chaperone dissociation from the subunits and promote subunit-subunit interactions [112]. In this study, we developed a fluorescence-based technique to determine the kinetics of usher-chaperone-subunit interactions. Here, we labeled the chaperone-subunit complexes with fluorescent probes to quantitatively measure the binding affinity of usher-chaperone-subunits by fluorometer analysis. The amine-reactive probe applied in these experiments can label the lysine residues and free amines of the proteins; however, there are limitations for the specificity of the amine reactive probe. Therefore, we can next use more specific probes such as thiol reactive probes to label cysteine residues of a protein. In this way, we can introduce a cysteine residue to the chaperone-subunit complexes which will be labeled by the thiol reactive probe. Currently, we constructed two PapD mutants, PapD N89C and PapD K112C. A set of cysteine-substitution mutants of PapC generated for a topology mapping study can also be used [137]. By similar analysis of fluorescence change by titrating with the unlabeled PapC, we can obtain Kd values from a set of analysis by specific labeling. The amine-reactive probe can label all the

lysine residue and free amine group, so the labeling is non-specific. However, using the thoil-reactive probe, we can engineer to label the specific residues and obtain the Kd values from the binding assay. These Kd values would be more accurate compared to Kd values from binding assays by non-specific labeling.

Our work presented here focuses on the function of PapC in recruitment of chaperone-subunit complexes and we developed the novel fluorescence based techniques as a quantitative tool to measure the usher-chaperone-subunit interactions. However, many molecular details of the function of the PapC usher in pilus biogenesis are unknown, so the new developed technique could be applied in further exploring the functions of PapC usher in the process of subunit polymerization or pilus translocation during pilus assembly.

In future experiments, fluorescence resonance energy transfer (FRET) will be also used to analyze kinetic binding of the usher and chaperone-subunit complexes. FRET takes advantage of an energy transfer mechanism between two fluorescent molecules. A fluorescent donor is excited at its specific excitation wavelength. Close contact between donor and a second molecule, acceptor, allow energy transfer from the donor to the acceptor molecule by a long-range dipole-dipole coupling mechanism, which leads to quenching of fluorescence emission of the donor molecule. Protein association curves can be drawn by measuring the decrease in fluorescence emission of the donor, which will allow us to quantitatively measure the interaction between a protein labeled with donor and a protein labeled with acceptor. We have a PapC mutant PapC 2insC in which a cysteine residue is inserted after the second residue of

the mature PapC. We can label PapC2insC with thiol reactive fluorescent donor and label chaperone-subunit $PapD_{N89C}$-subunit complexes with thiol reactive non-fluorescent acceptor so that we can analyze the binding of PapC NTD to chaperone-subunit. In this way, we could further analyze PapC mutants by placing the cysteine insertion at different locations and measure the binding affinity to different chaperone-subunit complexes. We could also use this quantitative assay to explore the catalytic function of PapC by calculate the binding rate of chaperone-subunit interactions or subunit-subunit interactions in the presence of WT PapC verse PapC mutants. In this way, we can find out the defective stage of mutant PapC during pilus assembly and determine the mechanisms of the usher in pilus biogenesis. Alternatively, by labeling one chaperone-subunit complex with the fluorescent donor molecule and labeling another chaperone-subunit complex with the non-fluorescent acceptor molecule and adding wild type PapC, the decrease in fluorescence can be measured to test the formation of subunit-subunit interactions at the usher. If the presence of the usher catalyzes subunit-subunit interactions, a faster rate of formation of subunit interactions will occur compared with chaperone-subunit complexes incubated without the usher. Similarly, by adding mutant PapC, we can measure the decrease in fluorescence to find out specific regions or residues of PapC which contribute to the catalytic role of the usher.

Structure of N- and C-terminal domain of PapC usher. Recently, the crystal structure of the $PapC_{130-640}$ usher central domain was solved. The crystal structures of

the NTD and CTD in the periplasm are required to provide more detail and to understand the functions of both domains. The structure of the NTD of FimD was solved and provided a snapshot of the NTD during type 1 pilus assembly (Fig. 1-4) [101]. However, the structures of the NTD and CTD in the P pilus system have not been solved. The full visualization of the crystal structure of both domains can help determine the relation with PapC central part, such as plug domain, β-5-6 hairpin and α-helix, which will help us understand the molecular details of pilus assembly the PapC usher. The detailed mechanism of the channel gating remains unknown and further experiments are required. *In vivo* antibiotic assays could be applied to the PapC mutants lacking plug domain, or plug domain with N- and C-terminal domains. We believe that the NTD and/or CTD might transduce the signal to trigger the displacement of plug domain to open the PapC channel upon binding to the chaperone-subunit complexes. We can use the antibiotics we used in this work to test the channel activity of the mutants PapC lacking different domains to understand the relations between NTD, CTD and plug domain. The molecular details of pilus assembly by the CTD remain unknown. A previous cryo-EM study showed that PapC assembles as a dimeric, twin-pore complex in the lipid [100]. In previous EM analysis, the wild type PapC and the mutant PapC lacking CTD were shown different twin pore packing. The PapC mutant lacking CTD twin pore dimer was shown to change the diameter in the 2D image and different monomer packing compared to the wild type [100]. This suggests that the CTD may be involved in the interface of the PapC dimer but is not required for the dimerization process. The EM study also showed that

electron density in the channel is weaker in the PapC mutant lacking the CTD [100], which indicates that the CTD might be positioned under the PapC channel. It is not known if the CTD directly contacts with the plug domain or β5-6 hairpin to trigger the conformational change of PapC upon chaperone-subunit targeting (Fig.1-3). It is proposed that after chaperone-subunit interaction with the NTD of PapC, a putative additional interaction between the adhesin and the CTD of PapC usher could cause the conformational change to the plug domain and/or β5-6 hairpin. The conformational change could, in turn, result in channel opening within PapC usher. Therefore, further experiments to solve the structure and function of the CTD and function are required to uncover the mechanism of the CTD in pilus biogenesis.

References

1. Stamm, W.E. and S.R. Norrby, *Urinary tract infections: disease panorama and challenges.* J Infect Dis, 2001. **183 Suppl 1**: p. S1-4.
2. Remaut, H., et al., *Fiber formation across the bacterial outer membrane by the chaperone/usher pathway.* Cell, 2008. **133**(4): p. 640-52.
3. Warren, J.W., et al., *Guidelines for antimicrobial treatment of uncomplicated acute bacterial cystitis and acute pyelonephritis in women. Infectious Diseases Society of America (IDSA).* Clin Infect Dis, 1999. **29**(4): p. 745-58.
4. Ng, T.W., et al., *The usher N terminus is the initial targeting site for chaperone-subunit complexes and participates in subsequent pilus biogenesis events.* J Bacteriol, 2004. **186**(16): p. 5321-31.
5. Johnson, J.R. and W.E. Stamm, *Urinary tract infections in women: diagnosis and treatment.* Ann Intern Med, 1989. **111**(11): p. 906-17.
6. Foxman, B. and P. Brown, *Epidemiology of urinary tract infections: transmission and risk factors, incidence, and costs.* Infect Dis Clin North Am, 2003. **17**(2): p. 227-41.
7. Karlowsky, J.A., et al., *Trends in antimicrobial resistance among urinary tract infection isolates of Escherichia coli from female outpatients in the United States.* Antimicrob Agents Chemother, 2002. **46**(8): p. 2540-5.
8. Medzhitov, R. and C. Janeway, Jr., *Innate immune recognition: mechanisms and pathways.* Immunol Rev, 2000. **173**: p. 89-97.
9. Marrs, C.F., et al., *Variations in 10 putative uropathogen virulence genes among urinary, faecal and peri-urethral Escherichia coli.* J Med Microbiol, 2002. **51**(2): p. 138-42.
10. Oelschlaeger, T.A., U. Dobrindt, and J. Hacker, *Virulence factors of uropathogens.* Curr Opin Urol, 2002. **12**(1): p. 33-8.
11. Engel, J.D. and A.J. Schaeffer, *Evaluation of and antimicrobial therapy for recurrent urinary tract infections in women.* Urol Clin North Am, 1998. **25**(4): p. 685-701, x.
12. Hooton, T.M., et al., *A prospective study of risk factors for symptomatic urinary tract infection in young women.* N Engl J Med, 1996. **335**(7): p. 468-74.
13. Cunningham, F.G. and M.J. Lucas, *Urinary tract infections complicating pregnancy.* Baillieres Clin Obstet Gynaecol, 1994. **8**(2): p. 353-73.
14. Nickel, J.C., *Management of urinary tract infections: historical perspective and current strategies: Part 2--Modern management.* J Urol, 2005. **173**(1): p. 27-32.
15. Wizemann, T.M., J.E. Adamou, and S. Langermann, *Adhesins as targets for vaccine development.* Emerg Infect Dis, 1999. **5**(3): p. 395-403.
16. Liu, Y., et al., *Cranberry changes the physicochemical surface properties of E. coli and adhesion with uroepithelial cells.* Colloids Surf B Biointerfaces, 2008.

65(1): p. 35-42.
17. Howell, A.B., *Cranberry proanthocyanidins and the maintenance of urinary tract health.* Crit Rev Food Sci Nutr, 2002. **42**(3 Suppl): p. 273-8.
18. Hacker, J. and J.B. Kaper, *Pathogenicity islands and the evolution of microbes.* Annu Rev Microbiol, 2000. **54**: p. 641-79.
19. Johnson, J.R. and T.A. Russo, *Extraintestinal pathogenic Escherichia coli: "the other bad E coli".* J Lab Clin Med, 2002. **139**(3): p. 155-62.
20. Johnson, J.R. and A.L. Stell, *Extended virulence genotypes of Escherichia coli strains from patients with urosepsis in relation to phylogeny and host compromise.* J Infect Dis, 2000. **181**(1): p. 261-72.
21. Jass, J., et al., *Physical properties of Escherichia coli P pili measured by optical tweezers.* Biophys J, 2004. **87**(6): p. 4271-83.
22. Bock, K., et al., *Specificity of binding of a strain of uropathogenic Escherichia coli to Gal alpha 1----4Gal-containing glycosphingolipids.* J Biol Chem, 1985. **260**(14): p. 8545-51.
23. Sokurenko, E.V., et al., *FimH family of type 1 fimbrial adhesins: functional heterogeneity due to minor sequence variations among fimH genes.* J Bacteriol, 1994. **176**(3): p. 748-55.
24. Bullitt, E. and L. Makowski, *Structural polymorphism of bacterial adhesion pili.* Nature, 1995. **373**(6510): p. 164-7.
25. Kuehn, M.J., et al., *P pili in uropathogenic E. coli are composite fibres with distinct fibrillar adhesive tips.* Nature, 1992. **356**(6366): p. 252-5.
26. Baga, M., M. Norgren, and S. Normark, *Biogenesis of E. coli Pap pili: papH, a minor pilin subunit involved in cell anchoring and length modulation.* Cell, 1987. **49**(2): p. 241-51.
27. Lund, B., et al., *The PapG protein is the alpha-D-galactopyranosyl-(1----4)-beta-D-galactopyranose-binding adhesin of uropathogenic Escherichia coli.* Proc Natl Acad Sci U S A, 1987. **84**(16): p. 5898-902.
28. Jones, C.H., et al., *FimH adhesin of type 1 pili is assembled into a fibrillar tip structure in the Enterobacteriaceae.* Proc Natl Acad Sci U S A, 1995. **92**(6): p. 2081-5.
29. Choudhury, D., et al., *X-ray structure of the FimC-FimH chaperone-adhesin complex from uropathogenic Escherichia coli.* Science, 1999. **285**(5430): p. 1061-6.
30. Bagg, A. and J.B. Neilands, *Molecular mechanism of regulation of siderophore-mediated iron assimilation.* Microbiol Rev, 1987. **51**(4): p. 509-18.
31. Neilands, J.B., A. Bindereif, and J.Z. Montgomerie, *Genetic basis of iron assimilation in pathogenic Escherichia coli.* Curr Top Microbiol Immunol, 1985. **118**: p. 179-95.
32. Williams, P.H., *Novel iron uptake system specified by ColV plasmids: an important component in the virulence of invasive strains of Escherichia coli.* Infect Immun, 1979. **26**(3): p. 925-32.

33. Orskov, I., C. Svanborg Eden, and F. Orskov, *Aerobactin production of serotyped Escherichia coli from urinary tract infections.* Med Microbiol Immunol, 1988. **177**(1): p. 9-14.
34. Marre, R., et al., *Contribution of cloned virulence factors from uropathogenic Escherichia coli strains to nephropathogenicity in an experimental rat pyelonephritis model.* Infect Immun, 1986. **54**(3): p. 761-7.
35. Keane, W.F., et al., *Mechanism of Escherichia coli alpha-hemolysin-induced injury to isolated renal tubular cells.* Am J Pathol, 1987. **126**(2): p. 350-7.
36. Gadeberg, O.V. and I. Orskov, *In vitro cytotoxic effect of alpha-hemolytic Escherichia coli on human blood granulocytes.* Infect Immun, 1984. **45**(1): p. 255-60.
37. Rennie, R.P. and J.P. Arbuthnott, *Partial characterisation of Escherichia coli haemolysin.* J Med Microbiol, 1974. **7**(2): p. 179-88.
38. Nieto, J.M., et al., *Suppression of transcription polarity in the Escherichia coli haemolysin operon by a short upstream element shared by polysaccharide and DNA transfer determinants.* Mol Microbiol, 1996. **19**(4): p. 705-13.
39. Bergstrom, T., et al., *Studies of urinary tract infections in infancy and childhood. XII. Eighty consecutive patients with neonatal infection.* J Pediatr, 1972. **80**(5): p. 858-66.
40. Aktories, K., *Rho proteins: targets for bacterial toxins.* Trends Microbiol, 1997. **5**(7): p. 282-8.
41. Mills, M., K.C. Meysick, and A.D. O'Brien, *Cytotoxic necrotizing factor type 1 of uropathogenic Escherichia coli kills cultured human uroepithelial 5637 cells by an apoptotic mechanism.* Infect Immun, 2000. **68**(10): p. 5869-80.
42. Koebnik, R., K.P. Locher, and P. Van Gelder, *Structure and function of bacterial outer membrane proteins: barrels in a nutshell.* Mol Microbiol, 2000. **37**(2): p. 239-53.
43. Thanassi, D.G. and S.J. Hultgren, *Multiple pathways allow protein secretion across the bacterial outer membrane.* Curr Opin Cell Biol, 2000. **12**(4): p. 420-30.
44. Andersen, C., C. Hughes, and V. Koronakis, *Protein export and drug efflux through bacterial channel-tunnels.* Curr Opin Cell Biol, 2001. **13**(4): p. 412-6.
45. Hueck, C.J., *Type III protein secretion systems in bacterial pathogens of animals and plants.* Microbiol Mol Biol Rev, 1998. **62**(2): p. 379-433.
46. Zhang, Y., et al., *Type III secretion decreases bacterial and host survival following phagocytosis of Yersinia pseudotuberculosis by macrophages.* Infect Immun, 2008. **76**(9): p. 4299-310.
47. Jacob-Dubuisson, F., R. Fernandez, and L. Coutte, *Protein secretion through autotransporter and two-partner pathways.* Biochim Biophys Acta, 2004. **1694**(1-3): p. 235-57.
48. Henderson, I.R., F. Navarro-Garcia, and J.P. Nataro, *The great escape: structure and function of the autotransporter proteins.* Trends Microbiol, 1998. **6**(9): p. 370-8.
49. Newman, C.L. and C. Stathopoulos, *Autotransporter and two-partner*

secretion: delivery of large-size virulence factors by gram-negative bacterial pathogens. Crit Rev Microbiol, 2004. **30**(4): p. 275-86.
50. Desvaux, M., N.J. Parham, and I.R. Henderson, *The autotransporter secretion system.* Res Microbiol, 2004. **155**(2): p. 53-60.
51. Desvaux, M., N.J. Parham, and I.R. Henderson, *Type V protein secretion: simplicity gone awry?* Curr Issues Mol Biol, 2004. **6**(2): p. 111-24.
52. Jacob-Dubuisson, F., C. Locht, and R. Antoine, *Two-partner secretion in Gram-negative bacteria: a thrifty, specific pathway for large virulence proteins.* Mol Microbiol, 2001. **40**(2): p. 306-13.
53. Thanassi, D.G., E.T. Saulino, and S.J. Hultgren, *The chaperone/usher pathway: a major terminal branch of the general secretory pathway.* Curr Opin Microbiol, 1998. **1**(2): p. 223-31.
54. Sandkvist, M., *Type II secretion and pathogenesis.* Infect Immun, 2001. **69**(6): p. 3523-35.
55. Cascales, E. and P.J. Christie, *The versatile bacterial type IV secretion systems.* Nat Rev Microbiol, 2003. **1**(2): p. 137-49.
56. Das, S. and K. Chaudhuri, *Identification of a unique IAHP (IcmF associated homologous proteins) cluster in Vibrio cholerae and other proteobacteria through in silico analysis.* In Silico Biol, 2003. **3**(3): p. 287-300.
57. Hsu, F., S. Schwarz, and J.D. Mougous, *TagR promotes PpkA-catalysed type VI secretion activation in Pseudomonas aeruginosa.* Mol Microbiol, 2009. **72**(5): p. 1111-25.
58. Binet, R., et al., *Protein secretion by Gram-negative bacterial ABC exporters--a review.* Gene, 1997. **192**(1): p. 7-11.
59. Koronakis, V., J. Eswaran, and C. Hughes, *Structure and function of TolC: the bacterial exit duct for proteins and drugs.* Annu Rev Biochem, 2004. **73**: p. 467-89.
60. Cornelis, G.R., *Yersinia type III secretion: send in the effectors.* J Cell Biol, 2002. **158**(3): p. 401-8.
61. Gauthier, A., N.A. Thomas, and B.B. Finlay, *Bacterial injection machines.* J Biol Chem, 2003. **278**(28): p. 25273-6.
62. Tardy, F., et al., *Yersinia enterocolitica type III secretion-translocation system: channel formation by secreted Yops.* Embo J, 1999. **18**(23): p. 6793-9.
63. Neyt, C. and G.R. Cornelis, *Insertion of a Yop translocation pore into the macrophage plasma membrane by Yersinia enterocolitica: requirement for translocators YopB and YopD, but not LcrG.* Mol Microbiol, 1999. **33**(5): p. 971-81.
64. Hakansson, S., et al., *The YopB protein of Yersinia pseudotuberculosis is essential for the translocation of Yop effector proteins across the target cell plasma membrane and displays a contact-dependent membrane disrupting activity.* Embo J, 1996. **15**(21): p. 5812-23.
65. d'Enfert, C., A. Ryter, and A.P. Pugsley, *Cloning and expression in Escherichia coli of the Klebsiella pneumoniae genes for production, surface localization and secretion of the lipoprotein pullulanase.* Embo J, 1987. **6**(11): p. 3531-8.

66. Stathopoulos, C., et al., *Secretion of virulence determinants by the general secretory pathway in gram-negative pathogens: an evolving story.* Microbes Infect, 2000. **2**(9): p. 1061-72.
67. Possot, O.M., M. Gerard-Vincent, and A.P. Pugsley, *Membrane association and multimerization of secreton component pulC.* J Bacteriol, 1999. **181**(13): p. 4004-11.
68. Pugsley, A.P., et al., *Recent progress and future directions in studies of the main terminal branch of the general secretory pathway in Gram-negative bacteria--a review.* Gene, 1997. **192**(1): p. 13-9.
69. Hardie, K.R., S. Lory, and A.P. Pugsley, *Insertion of an outer membrane protein in Escherichia coli requires a chaperone-like protein.* Embo J, 1996. **15**(5): p. 978-88.
70. Klauser, T., et al., *Characterization of the Neisseria Iga beta-core. The essential unit for outer membrane targeting and extracellular protein secretion.* J Mol Biol, 1993. **234**(3): p. 579-93.
71. Oomen, C.J., et al., *Structure of the translocator domain of a bacterial autotransporter.* Embo J, 2004. **23**(6): p. 1257-66.
72. Thanassi, D.G., et al., *Protein secretion in the absence of ATP: the autotransporter, two-partner secretion and chaperone/usher pathways of gram-negative bacteria (review).* Mol Membr Biol, 2005. **22**(1-2): p. 63-72.
73. Oliver, D.C., G. Huang, and R.C. Fernandez, *Identification of secretion determinants of the Bordetella pertussis BrkA autotransporter.* J Bacteriol, 2003. **185**(2): p. 489-95.
74. Maurer, J., J. Jose, and T.F. Meyer, *Characterization of the essential transport function of the AIDA-I autotransporter and evidence supporting structural predictions.* J Bacteriol, 1999. **181**(22): p. 7014-20.
75. Jacob-Dubuisson, F., et al., *First structural insights into the TpsB/Omp85 superfamily.* Biol Chem, 2009. **390**(8): p. 675-84.
76. Guedin, S., et al., *Novel topological features of FhaC, the outer membrane transporter involved in the secretion of the Bordetella pertussis filamentous hemagglutinin.* J Biol Chem, 2000. **275**(39): p. 30202-10.
77. Makhov, A.M., et al., *Filamentous hemagglutinin of Bordetella pertussis. A bacterial adhesin formed as a 50-nm monomeric rigid rod based on a 19-residue repeat motif rich in beta strands and turns.* J Mol Biol, 1994. **241**(1): p. 110-24.
78. Ding, Z. and P.J. Christie, *Agrobacterium tumefaciens twin-arginine-dependent translocation is important for virulence, flagellation, and chemotaxis but not type IV secretion.* J Bacteriol, 2003. **185**(3): p. 760-71.
79. Kostakioti, M., et al., *Mechanisms of protein export across the bacterial outer membrane.* J Bacteriol, 2005. **187**(13): p. 4306-14.
80. Christie, P.J., et al., *A gene required for transfer of T-DNA to plants encodes an ATPase with autophosphorylating activity.* Proc Natl Acad Sci U S A, 1989. **86**(24): p. 9677-81.
81. Sexton, J.A., et al., *Legionella pneumophila DotU and IcmF are required for*

stability of the Dot/Icm complex. Infect Immun, 2004. **72**(10): p. 5983-92.
82. Pukatzki, S., et al., *Identification of a conserved bacterial protein secretion system in Vibrio cholerae using the Dictyostelium host model system.* Proc Natl Acad Sci U S A, 2006. **103**(5): p. 1528-33.
83. Schell, M.A., et al., *Type VI secretion is a major virulence determinant in Burkholderia mallei.* Mol Microbiol, 2007. **64**(6): p. 1466-85.
84. Mougous, J.D., et al., *A virulence locus of Pseudomonas aeruginosa encodes a protein secretion apparatus.* Science, 2006. **312**(5779): p. 1526-30.
85. Zheng, J. and K.Y. Leung, *Dissection of a type VI secretion system in Edwardsiella tarda.* Mol Microbiol, 2007. **66**(5): p. 1192-206.
86. Bladergroen, M.R., K. Badelt, and H.P. Spaink, *Infection-blocking genes of a symbiotic Rhizobium leguminosarum strain that are involved in temperature-dependent protein secretion.* Mol Plant Microbe Interact, 2003. **16**(1): p. 53-64.
87. James, D., et al., *The Actinobacillus actinomycetemcomitans ribose binding protein RbsB interacts with cognate and heterologous autoinducer 2 signals.* Infect Immun, 2006. **74**(7): p. 4021-9.
88. Wimley, W.C., *The versatile beta-barrel membrane protein.* Curr Opin Struct Biol, 2003. **13**(4): p. 404-11.
89. Bos, M.P. and J. Tommassen, *Biogenesis of the Gram-negative bacterial outer membrane.* Curr Opin Microbiol, 2004. **7**(6): p. 610-6.
90. Mogensen, J.E. and D.E. Otzen, *Interactions between folding factors and bacterial outer membrane proteins.* Mol Microbiol, 2005. **57**(2): p. 326-46.
91. Bulieris, P.V., et al., *Folding and insertion of the outer membrane protein OmpA is assisted by the chaperone Skp and by lipopolysaccharide.* J Biol Chem, 2003. **278**(11): p. 9092-9.
92. Rouviere, P.E. and C.A. Gross, *SurA, a periplasmic protein with peptidyl-prolyl isomerase activity, participates in the assembly of outer membrane porins.* Genes Dev, 1996. **10**(24): p. 3170-82.
93. Bitto, E. and D.B. McKay, *Binding of phage-display-selected peptides to the periplasmic chaperone protein SurA mimics binding of unfolded outer membrane proteins.* FEBS Lett, 2004. **568**(1-3): p. 94-8.
94. Manting, E.H. and A.J. Driessen, *Escherichia coli translocase: the unravelling of a molecular machine.* Mol Microbiol, 2000. **37**(2): p. 226-38.
95. Thanassi, D.G., *Ushers and secretins: channels for the secretion of folded proteins across the bacterial outer membrane.* J Mol Microbiol Biotechnol, 2002. **4**(1): p. 11-20.
96. Nikaido, H., *Molecular basis of bacterial outer membrane permeability revisited.* Microbiol Mol Biol Rev, 2003. **67**(4): p. 593-656.
97. Thanassi, D.G., et al., *The PapC usher forms an oligomeric channel: implications for pilus biogenesis across the outer membrane.* Proc Natl Acad Sci U S A, 1998. **95**(6): p. 3146-51.
98. Nishiyama, M., et al., *Identification and characterization of the chaperone-subunit complex-binding domain from the type 1 pilus assembly*

platform FimD. J Mol Biol, 2003. **330**(3): p. 513-25.
99. Thanassi, D.G., et al., *Bacterial outer membrane ushers contain distinct targeting and assembly domains for pilus biogenesis.* J Bacteriol, 2002. **184**(22): p. 6260-9.
100. Li, H., et al., *The outer membrane usher forms a twin-pore secretion complex.* J Mol Biol, 2004. **344**(5): p. 1397-407.
101. Nishiyama, M., et al., *Structural basis of chaperone-subunit complex recognition by the type 1 pilus assembly platform FimD.* Embo J, 2005. **24**(12): p. 2075-86.
102. Li, H. and D.G. Thanassi, *Use of a combined cryo-EM and X-ray crystallography approach to reveal molecular details of bacterial pilus assembly by the chaperone/usher pathway.* Curr Opin Microbiol, 2009. **12**(3): p. 326-32.
103. Eisenstein, B.I., *Phase variation of type 1 fimbriae in Escherichia coli is under transcriptional control.* Science, 1981. **214**(4518): p. 337-9.
104. van der Woude, M., B. Braaten, and D. Low, *Epigenetic phase variation of the pap operon in Escherichia coli.* Trends Microbiol, 1996. **4**(1): p. 5-9.
105. Olsen, P.B. and P. Klemm, *Localization of promoters in the fim gene cluster and the effect of H-NS on the transcription of fimB and fimE.* FEMS Microbiol Lett, 1994. **116**(1): p. 95-100.
106. Gally, D.L., J. Leathart, and I.C. Blomfield, *Interaction of FimB and FimE with the fim switch that controls the phase variation of type 1 fimbriae in Escherichia coli K-12.* Mol Microbiol, 1996. **21**(4): p. 725-38.
107. Pugsley, A.P., *The complete general secretory pathway in gram-negative bacteria.* Microbiol Rev, 1993. **57**(1): p. 50-108.
108. Jones, C.H., et al., *The chaperone-assisted membrane release and folding pathway is sensed by two signal transduction systems.* Embo J, 1997. **16**(21): p. 6394-406.
109. Zavialov, A.V., et al., *Structure and biogenesis of the capsular F1 antigen from Yersinia pestis: preserved folding energy drives fiber formation.* Cell, 2003. **113**(5): p. 587-96.
110. Sauer, F.G., et al., *Chaperone priming of pilus subunits facilitates a topological transition that drives fiber formation.* Cell, 2002. **111**(4): p. 543-51.
111. Sauer, F.G., et al., *Structural basis of chaperone function and pilus biogenesis.* Science, 1999. **285**(5430): p. 1058-61.
112. Nishiyama, M., et al., *Reconstitution of pilus assembly reveals a bacterial outer membrane catalyst.* Science, 2008. **320**(5874): p. 376-9.
113. Norgren, M., et al., *Nucleotide sequence, regulation and functional analysis of the papC gene required for cell surface localization of Pap pili of uropathogenic Escherichia coli.* Mol Microbiol, 1987. **1**(2): p. 169-78.
114. Jacob-Dubuisson, F., R. Striker, and S.J. Hultgren, *Chaperone-assisted self-assembly of pili independent of cellular energy.* J Biol Chem, 1994. **269**(17): p. 12447-55.

115. Vetsch, M., et al., *Mechanism of fibre assembly through the chaperone-usher pathway.* EMBO Rep, 2006. **7**(7): p. 734-8.
116. Remaut, H., et al., *Donor-strand exchange in chaperone-assisted pilus assembly proceeds through a concerted beta strand displacement mechanism.* Mol Cell, 2006. **22**(6): p. 831-42.
117. Zavialov, A.V., et al., *Resolving the energy paradox of chaperone/usher-mediated fibre assembly.* Biochem J, 2005. **389**(Pt 3): p. 685-94.
118. So, S.S. and D.G. Thanassi, *Analysis of the requirements for pilus biogenesis at the outer membrane usher and the function of the usher C-terminus.* Mol Microbiol, 2006. **60**(2): p. 364-75.
119. Saulino, E.T., et al., *Ramifications of kinetic partitioning on usher-mediated pilus biogenesis.* Embo J, 1998. **17**(8): p. 2177-85.
120. Dodson, K.W., et al., *Outer-membrane PapC molecular usher discriminately recognizes periplasmic chaperone-pilus subunit complexes.* Proc Natl Acad Sci U S A, 1993. **90**(8): p. 3670-4.
121. Datsenko, K.A. and B.L. Wanner, *One-step inactivation of chromosomal genes in Escherichia coli K-12 using PCR products.* Proc Natl Acad Sci U S A, 2000. **97**(12): p. 6640-5.
122. Holden, N., et al., *Regulation of P-fimbrial phase variation frequencies in Escherichia coli CFT073.* Infect Immun, 2007. **75**(7): p. 3325-34.
123. Philip, F. and S. Scarlata, *Real-time measurements of protein affinities on membrane surfaces by fluorescence spectroscopy.* Sci STKE, 2006. **2006**(350): p. pl5.
124. Grant, S.G., et al., *Differential plasmid rescue from transgenic mouse DNAs into Escherichia coli methylation-restriction mutants.* Proc Natl Acad Sci U S A, 1990. **87**(12): p. 4645-9.
125. Baneyx, F. and G. Georgiou, *In vivo degradation of secreted fusion proteins by the Escherichia coli outer membrane protease OmpT.* J Bacteriol, 1990. **172**(1): p. 491-4.
126. Blomfield, I.C., M.S. McClain, and B.I. Eisenstein, *Type 1 fimbriae mutants of Escherichia coli K12: characterization of recognized afimbriate strains and construction of new fim deletion mutants.* Mol Microbiol, 1991. **5**(6): p. 1439-45.
127. Hultgren, S.J., et al., *The PapG adhesin of uropathogenic Escherichia coli contains separate regions for receptor binding and for the incorporation into the pilus.* Proc Natl Acad Sci U S A, 1989. **86**(12): p. 4357-61.
128. Mapingire, O.S., et al., *Modulating effects of the plug, helix and N- and C-terminal domains on channel properties of the PapC usher.* J Biol Chem, 2009.
129. Tewari, R., et al., *The PapG tip adhesin of P fimbriae protects Escherichia coli from neutrophil bactericidal activity.* Infect Immun, 1994. **62**(12): p. 5296-304.
130. Cherepanov, P.P. and W. Wackernagel, *Gene disruption in Escherichia coli:*

TcR and KmR cassettes with the option of Flp-catalyzed excision of the antibiotic-resistance determinant. Gene, 1995. **158**(1): p. 9-14.
131. Lee, Y.M., K.W. Dodson, and S.J. Hultgren, *Adaptor function of PapF depends on donor strand exchange in P-pilus biogenesis of Escherichia coli.* J Bacteriol, 2007. **189**(14): p. 5276-83.
132. Rose, R.J., et al., *Unraveling the molecular basis of subunit specificity in P pilus assembly by mass spectrometry.* Proc Natl Acad Sci U S A, 2008. **105**(35): p. 12873-8.
133. Langermann, S., et al., *Prevention of mucosal Escherichia coli infection by FimH-adhesin-based systemic vaccination.* Science, 1997. **276**(5312): p. 607-11.
134. Connell, I., et al., *Type 1 fimbrial expression enhances Escherichia coli virulence for the urinary tract.* Proc Natl Acad Sci U S A, 1996. **93**(18): p. 9827-32.
135. Lindberg, F.P., B. Lund, and S. Normark, *Genes of pyelonephritogenic E. coli required for digalactoside-specific agglutination of human cells.* Embo J, 1984. **3**(5): p. 1167-73.
136. Jacob-Dubuisson, F., et al., *Initiation of assembly and association of the structural elements of a bacterial pilus depend on two specialized tip proteins.* Embo J, 1993. **12**(3): p. 837-47.
137. Henderson, N.S., et al., *Topology of the outer membrane usher PapC determined by site-directed fluorescence labeling.* J Biol Chem, 2004. **279**(51): p. 53747-54.
138. Hahn, E., et al., *Exploring the 3D molecular architecture of Escherichia coli type 1 pili.* J Mol Biol, 2002. **323**(5): p. 845-57.
139. Pages, J.M., C.E. James, and M. Winterhalter, *The porin and the permeating antibiotic: a selective diffusion barrier in Gram-negative bacteria.* Nat Rev Microbiol, 2008. **6**(12): p. 893-903.
140. Ceccarelli, M. and P. Ruggerone, *Physical insights into permeation of and resistance to antibiotics in bacteria.* Curr Drug Targets, 2008. **9**(9): p. 779-88.
141. Nikaido, H. and M. Vaara, *Molecular basis of bacterial outer membrane permeability.* Microbiol Rev, 1985. **49**(1): p. 1-32.
142. Nikaido, H. and E.Y. Rosenberg, *Porin channels in Escherichia coli: studies with liposomes reconstituted from purified proteins.* J Bacteriol, 1983. **153**(1): p. 241-52.
143. Gong, M. and L. Makowski, *Helical structure of P pili from Escherichia coli. Evidence from X-ray fiber diffraction and scanning transmission electron microscopy.* J Mol Biol, 1992. **228**(3): p. 735-42.
144. Nakae, T., *Identification of the outer membrane protein of E. coli that produces transmembrane channels in reconstituted vesicle membranes.* Biochem Biophys Res Commun, 1976. **71**(3): p. 877-84.
145. Nakae, T., *Outer membrane of Salmonella. Isolation of protein complex that produces transmembrane channels.* J Biol Chem, 1976. **251**(7): p. 2176-8.
146. Soto, G.E., et al., *Periplasmic chaperone recognition motif of subunits*

mediates quaternary interactions in the pilus. Embo J, 1998. **17**(21): p. 6155-67.